



Contents lists available at ScienceDirect

## Linear Algebra and its Applications

journal homepage: [www.elsevier.com/locate/laa](http://www.elsevier.com/locate/laa)

# Eigenvalue superposition for Toeplitz matrix-sequences with matrix order dependent symbols

M. Bogoya<sup>a,\*</sup>, S.M. Grudsky<sup>b,c</sup>, S. Serra-Capizzano<sup>d,e</sup><sup>a</sup> *Departamento de Matemáticas, Universidad del Valle, Cali, Colombia*<sup>b</sup> *Departamento de Matemáticas, CINVESTAV del IPN, Mexico D.F., Mexico*<sup>c</sup> *Regional Mathematical Center, Southern Federal University, Rostov-on-Don, Russia*<sup>d</sup> *Dipartimento di Scienza e Alta Tecnologia, University of Insubria, Como, Italy*<sup>e</sup> *Dept. of Information Technology, University of Uppsala, Uppsala, Sweden*

## ARTICLE INFO

*Article history:*

Received 6 November 2023

Received in revised form 31 March 2024

Accepted 19 April 2024

Available online 24 April 2024

Submitted by T. Ehrhardt

For the 70th years of Prof. Albrecht Böttcher, thanking him for many years of friendship and of continuous mathematical inspiration

*MSC:*

primary 15B05, 65F15, 47B35

secondary 15A18, 47A38

*Keywords:*

Eigenvalue expansion

Toeplitz matrix

Asymptotic expansion

Matrix-less method

## ABSTRACT

The eigenvalues of Toeplitz matrices  $T_n(f)$  with a real-valued generating function  $f$ , satisfying some conditions and tracing out a simple loop over the interval  $[-\pi, \pi]$ , are known to admit an asymptotic expansion with the form

$$\lambda_j(T_n(f)) = f(\sigma_{j,n}) + c_1(\sigma_{j,n})h + c_2(\sigma_{j,n})h^2 + O(h^3),$$

where  $h = 1/(n+1)$ ,  $\sigma_{j,n} = \pi j h$ , and  $c_k$  are some bounded coefficients depending only on  $f$ . The numerical results presented in the literature suggest that the effective conditions for the expansion to hold are weaker and reduce to a fixed smoothness and to having only two intervals of monotonicity over  $[-\pi, \pi]$ .

In this article we investigate the superposition caused over this expansion, when considering the following linear combination

$$\lambda_j(T_n(f_0) + \beta_{n,1}T_n(f_1) + \beta_{n,2}T_n(f_2)),$$

\* Corresponding author.

*E-mail addresses:* [johan.bogoya@correounivalle.edu.co](mailto:johan.bogoya@correounivalle.edu.co) (M. Bogoya), [grudsky@math.cinvestav.mx](mailto:grudsky@math.cinvestav.mx) (S.M. Grudsky), [s.serracapizzano@uninsubria.it](mailto:s.serracapizzano@uninsubria.it) (S. Serra-Capizzano).

where  $\beta_{n,1}, \beta_{n,2}$  are certain constants depending on  $n$  and the generating functions  $f_0, f_1, f_2$  are either simple loop or satisfy the weaker conditions mentioned before.

We formally obtain an asymptotic expansion in this setting under simple-loop related assumptions, and we show numerically that there is much more to investigate, opening the door to linear in time algorithms for the computation of eigenvalues of large matrices of this type including a multilevel setting.

The problem is of concrete interest, considering spectral features of matrices stemming from the numerical approximation of standard differential operators and distributed order fractional differential equations, via local methods such as Finite Differences, Finite Elements, and Isogeometric Analysis.

© 2024 The Authors. Published by Elsevier Inc. This is an open access article under the CC BY-NC-ND license (<http://creativecommons.org/licenses/by-nc-nd/4.0/>).

---

## 1. Introduction and preliminaries

The current section is divided into three parts, all of introductory type. In Subsection 1.1, we introduce notations, definitions, and preliminary results concerning Toeplitz structures, which are essential for the mathematical formulation of the problem and its technical solution.

In Subsection 1.2, we present a standard introduction to the considered problem and we consider its connections with the previous literature, with special attention to the simple loop method (see [1,2]) and to the matrix-less solvers. Indeed, beside the technical results, which are mathematically non trivial, the new findings have application to the design of fast eigensolvers of matrix-less type (see [3,4] and references therein) for the computation in linear time of the eigenvalues of large matrices, stemming e.g. from the numerical approximation via local methods, like Finite Differences, Finite Elements, and Isogeometric Analysis (see [5–7] and references there reported), of coercive differential equations like diffusion-advection, or from distributed order fractional differential equations again approximated using local methods (see [8–10] and references therein). The same info can be used, in connections with the notions of GLT/Toeplitz momentary symbols [11,12] including in a multilevel setting.

In Subsection 1.3, we also present a brief account on the theory of Generalized Locally Toeplitz (GLT) matrix-sequences [13–17] and on the notion of GLT momentary symbols [12,18], which are of support in interpreting our findings from a different perspective.

The rest of the paper is organized as follows. In Section 2 we present the main results, while in Section 3 the related proofs are given. Section 4 is devoted to numerical experiments, showing the potential of the given matrix-less eigensolvers. Finally, in Section 5, conclusions, open problems, and future promising developments are illustrated, emphasizing the challenging connections with the notion of GLT momentary symbols (see [12,18]).

1.1. Preliminaries

For a complex or real sequence  $(a_j)_{j=-\infty}^{\infty}$ , we consider the Toeplitz matrix

$$[a_{i-j}]_{i,j=1}^n = \begin{bmatrix} a_0 & a_{-1} & a_{-2} & \cdots & \cdots & a_{-(n-1)} \\ a_1 & \ddots & \ddots & \ddots & & \vdots \\ a_2 & \ddots & \ddots & \ddots & \ddots & \vdots \\ \vdots & \ddots & \ddots & \ddots & \ddots & a_{-2} \\ \vdots & & \ddots & \ddots & \ddots & a_{-1} \\ a_{n-1} & \cdots & \cdots & a_2 & a_1 & a_0 \end{bmatrix},$$

which is characterized from the fact to show constant entries along each diagonal parallel to the main one. When taking a function  $f: [-\pi, \pi] \rightarrow \mathbb{C}$  belonging to  $L^1([-\pi, \pi])$ , the  $n$ th Toeplitz matrix generated by  $f$  is formally expressed as

$$T_n(f) \equiv [a_{i-j}(f)]_{i,j=1}^n,$$

where the quantities  $a_k(f)$  are the Fourier coefficients of  $f$ ,

$$a_k(f) \equiv \frac{1}{2\pi} \int_{-\pi}^{\pi} f(\sigma) e^{-ik\sigma} d\sigma, \quad k \in \mathbb{Z}.$$

In order to fix the terminology, we refer to  $\{T_n(f)\}_n$  as the Toeplitz sequence generated by  $f$ , which in turn is called the *generating function* of  $\{T_n(f)\}_n$ : we remind that the notion of symbol is a different notion recalled in Definition 1.1 and the classical results for Toeplitz matrix-sequences are reported in Theorem 1.1. If the generating function  $f$  is real-valued, then all the matrices  $T_n(f)$  are Hermitian and their spectral properties are known in detail, from the localization of the eigenvalues to the asymptotic spectral distribution in the Weyl sense; see Definition 1.1, Theorem 1.1, [16,19] and the references therein.

In the current work, we focus on the case where  $f$  is simple-loop or real-valued and showing an infinite cosine expansion, that is, a function of the form

$$f(\sigma) = f_0 + 2 \sum_{k=1}^m f_k \cos(k\sigma), \quad f_0, f_1, \dots, f_m \in \mathbb{R}, \quad m \in \mathbb{N} \cup \{\infty\},$$

so that  $f(2\pi - s) = f(s)$ . We say that a cosine expansion function is monotone if it is either increasing or decreasing over the interval  $[0, \pi]$ . The banded Toeplitz matrix generated by  $f$  is the real symmetric matrix given by



When approximating the operator  $(-1)^q \frac{d^{2q}}{dx^{2q}}$ ,  $q = 0, 1, 2, \dots$ , on a given interval with proper boundary conditions and a uniform gridding, we end up with structures either as  $T_n(f_q)$  with  $f_q$  being a monotone, real-valued cosine polynomial of the form

$$f_q(\sigma) = (2 - 2 \cos(\sigma))^q, \quad q = 0, 1, 2, \dots, \tag{1.2}$$

if one uses centered Finite Differences of precision order 2 [7], or as  $T_n(g_q)$  with  $g_q$  being a real-valued cosine polynomial of the form

$$g_q(\sigma) = (2 - 2 \cos(\sigma))^q p_q(\sigma), \quad q = 0, 1, 2, \dots, \tag{1.3}$$

where  $p_q$  is a strictly positive cosine polynomial, when using Isogeometric Analysis with maximal regularity [6,26]. We recall that the considered Finite Differences are characterized by  $O(h^2)$  precision and minimal bandwidth, while in the case of (1.3) the bandwidth is larger, but a much higher precision is obtained as described in [6].

Unfortunately, for these generating functions the requirement that  $f''(0) > 0$  is not satisfied if  $q \neq 1$ . Recently, in [27] the SLM was extended for a generating function with  $f''(0) = \infty$  but with an expansion valid only for the inner eigenvalues. Actually, based on numerical experiments, it was conjectured that an expansion similar to (1.1) holds at least for the inner eigenvalues and all monotone cosine trigonometric polynomials  $f$ . Moreover, Barrera, Böttcher, Grudsky, and Maximenko [28,29] formally studied the case  $q = 2$ . In [30] the authors extended SLM to the case where the generating function has a minimum of order 4.

In [1, Ch 7], Böttcher briefly mentioned that the asymptotic expansion (1.1) can be used to compute an accurate approximation of  $\lambda_j(T_n(f))$  for every sufficiently large  $n$ , provided the values  $\lambda_{j_1}(T_{n_1}(f))$ ,  $\lambda_{j_2}(T_{n_2}(f))$ ,  $\lambda_{j_3}(T_{n_3}(f))$  are available for moderately sized  $n_1, n_2, n_3$  with  $\sigma_{j_1, n_1} = \sigma_{j_2, n_2} = \sigma_{j_3, n_3} = \sigma_{j, n}$ . The idea has evolved in [3,4,20] and highly accurate matrix-less methods of optimal linear cost have been developed. A wide set of numerical experiments has been reported, accompanied by an appropriate error analysis. It should be stressed that in essence the matrix-less algorithms are completely analogous to the extrapolation procedure, which is employed in the context of Romberg integration for obtaining high precision approximations of an integral from a few coarse trapezoidal approximations [31, Ch 3.4]. In this regard, the asymptotic expansion (1.1) plays here the same role as the Euler–Maclaurin summation formula [31, Ch 3.3].

To give an idea of the extrapolation process in this setting, consider the expansion (1.1) and fix  $r, s \in [0, \pi]$  such that  $r < s$  and

$$\begin{aligned} r &= \frac{j_{0,r}\pi}{n_0 + 1} = \frac{j_{1,r}\pi}{n_1 + 1} = \frac{j_r\pi}{n + 1}, \\ s &= \frac{j_{0,s}\pi}{n_0 + 1} = \frac{j_{1,s}\pi}{n_1 + 1} = \frac{j_s\pi}{n + 1}, \\ h_1 &= \frac{1}{2}h_0, \quad h_0 = \frac{j_{0,r}}{n_0 + 1}, \quad h_1 = \frac{j_{1,r}}{n_1 + 1}, \end{aligned}$$

$$h \ll h_1, \quad h = \frac{j_r}{n + 1},$$

that is  $n \gg n_1 > n_0$ . We show with a basic example how to use formula (1.1) at sizes  $n_0, n_1$ , for getting an improved approximation of all the eigenvalues at size  $n \gg n_i$ ,  $i = 0, 1$ . We first compute  $\lambda_{j_0,u}(T_{n_0}(f))$  and  $\lambda_{j_1,u}(T_{n_1}(f))$ ,  $u = r, s$ , with sufficient high precision. Then use the formula for canceling out terms and approximating  $c_1(u), c_2(u)$  for  $u = r, s$ , namely we compute

$$\begin{aligned} q_1(u) &= \frac{2}{h_0^2} [\lambda_{j_0,u}(T_{n_0}(f)) - 2\lambda_{j_1,u}(T_{n_1}(f))] = c_2(u) + O(h_0), \\ q_2(u) &= \frac{2}{h_0} [\lambda_{j_0,u}(T_{n_0}(f)) - \lambda_{j_1,u}(T_{n_1}(f))] - \frac{3h_0}{4} q_1(u) = c_1(u) + O(h_0^2). \end{aligned}$$

Now we replace these approximations of  $c_1(u), c_2(u)$ ,  $u = 1, 2$ , in relation (1.1) for the large value  $n$ , obtaining an approximation of

$$\lambda_{j_u}(T_n(f)),$$

with an error of the form  $O(h_0^2 h + h_0 h^2 + h^3)$ . For the inner eigenvalues, that is, those with  $j$  such that  $j_r < j < j_s$ , interpolation can be used and this gives a clear understanding of the reason why Ekström and Garoni called the corresponding matrix-less algorithm of “extrapolation-interpolation” type [3].

Here we are interested in extending the machinery, both theoretically and computationally, to the more involved case of linear combinations of matrix-order depending generating functions, see (1.4), with the following two targets:

- proving formally the asymptotic expansions;
- giving related matrix-less procedures.

### 1.2. The problem and the literature

As already mentioned in Subsection 1.1, we investigate the superposition caused over the expansion (1.1), when considering the following linear combination

$$\lambda_j(T_n(f_0 + \beta_{n,1}f_1 + \beta_{n,2}f_2)), \tag{1.4}$$

where  $\beta_{n,1}, \beta_{n,2}$  are certain constants depending on  $n$ , and the generating functions  $f_0, f_1, f_2$  are either of simple-loop type or satisfy some weaker conditions. More specifically, when  $\beta_{n,1} = h, h^h, \beta_{n,2} = 0$ , and  $f_j$  ( $j = 0, 1$ ) are simple-loop, we formally extend the simple-loop method to this setting obtaining an asymptotic expansion in the same fashion of (1.1): we emphasize that the case  $\beta_{n,1} = h^h$  is related to the approximation of distributed fraction equations (see [9,10] and references therein). When  $\beta_{n,1} = \alpha_1 h^2$  and  $\beta_{n,2} = \alpha_2 h^4, \alpha_1, \alpha_2 \in \mathbb{R}$ , and  $f_j$  ( $j = 1, 2, 3$ ) are certain real-valued cosine polynomials,

we show numerically that (1.1) still works. As a consequence, our findings show that there is much more to investigate, opening the door to linear in time algorithms for the computation of eigenvalues of large matrices of this type.

The problem is of great interest in applications, when considering spectral features of matrices stemming from the numerical approximation of standard differential operators [12,32] and distributed order fractional differential equations [9,10,33,34]. In particular, for standard differential operators, our approach could be very promising for any local approximation technique of integro-differential operators, giving rise to GLT matrix-sequences (see [14–17] and references therein), with special attention to the case of Finite Elements [5] and Isogeometric analysis, both with maximal regularity and intermediate regularity [6].

Furthermore, from a theoretical viewpoint, it is worth stressing that it is the first time that an eigenvalue expansion is theoretically obtained for a Toeplitz matrix-sequence with a generating function depending on  $n$ .

In the next steps we introduce the essentials of the GLT theory (see [13–17] and references therein) and of the new concept of GLT momentary symbols [18], related to matrix structures as those appearing in (1.4).

### 1.3. GLT theory and GLT momentary symbols

In this technical part we give the essentials of the GLT theory. We start with the definition of spectral symbol and of symbol (in the singular value sense). Then we give part of the axioms that characterize the GLT matrix-sequences and we spend a few words on the new concept of GLT momentary symbols.

**Definition 1.1.** Let  $f: D \rightarrow \mathbb{C}$  be a measurable function defined on the Lebesgue measurable set  $D$  of positive and finite measure. Assume that  $\{A_n\}_n$  is a sequence of matrices such that  $A_n$  is of size  $d_n \times d_n$ ,  $d_n \rightarrow \infty$ , as  $n \rightarrow \infty$  and with eigenvalues  $\lambda_j(A_n)$  and singular values  $\sigma_j(A_n)$ ,  $j = 1, \dots, d_n$ .

- We say that  $\{A_n\}_n$  is *distributed as  $f$  over  $D$  in the sense of the eigenvalues*, and we write  $\{A_n\}_n \sim_\lambda (f, D)$ , if

$$\lim_{n \rightarrow \infty} \frac{1}{d_n} \sum_{j=1}^{d_n} F(\lambda_j(A_n)) = \frac{1}{\mu(D)} \int_D F(f(t)) dt, \tag{1.5}$$

for every continuous function  $F$  with compact support. In this case, we say that  $f$  is the *spectral symbol* of  $\{A_n\}_n$ .

- We say that  $\{A_n\}_n$  is *distributed as  $f$  over  $D$  in the sense of the singular values*, and we write  $\{A_n\}_p \sim_\sigma (f, D)$ , if

$$\lim_{n \rightarrow \infty} \frac{1}{d_n} \sum_{j=1}^{d_n} F(\sigma_j(A_n)) = \frac{1}{\mu(D)} \int_D F(|f(t)|) dt, \tag{1.6}$$

for every continuous function  $F$  with compact support. In this case, we say that  $f$  is the *symbol* of  $\{A_n\}_n$  in the sense of the singular values. In the case where  $f \equiv 0$ , i.e.  $\{A_n\}_n \sim_\sigma 0$  for any admissible domain  $D$ , the related matrix-sequence is called *zero-distributed matrix-sequence*.

Throughout the paper, when the domain can be easily inferred from the context, we replace the notation  $\{A_n\}_n \sim_{\lambda, \sigma} (f, D)$  with  $\{A_n\}_n \sim_{\lambda, \sigma} f$ . A noteworthy result due to Tilli [35] and Tyrtshnikov and Zamarashkin [36] is the following.

**Theorem 1.1.** *Let  $f \in L^1([-\pi, \pi])$ , then  $\{T_n(f)\}_n \sim_\sigma (f, [-\pi, \pi])$ . If  $f$  is a real-valued function almost everywhere, then  $\{T_n(f)\}_n \sim_\lambda (f, [-\pi, \pi])$ .*

It is worth mentioning that historically Toeplitz finite sections were studied since the beginning of the twentieth century (see e.g. the book by Böttcher and Silbermann [19] and its predecessors), with special emphasis on the case where the generating function  $f$  is essentially bounded, then Tilli defined the much larger space of the Locally Toeplitz matrix-sequences [37], which includes banded variable Toeplitz matrix-sequences and standard Toeplitz matrix-sequences with  $L^2$  generating functions. The extension to the GLT class [38,39] defines a maximal  $*$ -algebra of matrix-sequences, as proven by Barbarino et al. [14,15], which includes the Toeplitz matrix-sequences with  $L^1$  generating functions, and which turns out to be isometrically equivalent to the measurable functions on  $[0, 1] \times [-\pi, \pi]$  [40]. Finally the notion of GLT momentary symbols is useful especially in a computational framework for fast eigenvalue solvers.

In the sequel, we introduce the GLT class, a  $*$ -algebra of matrix-sequences containing Toeplitz matrix-sequences. The formal definition of GLT matrix-sequences is rather technical and can be found in the scalar unilevel, scalar multilevel, block unilevel, and block multilevel in the following books and review papers [14–17], respectively. The original construction is involved and needs a whole coherent set of definitions and mathematical objects; see [37–39]. However, in the writing of the books and the reviews, the authors realized that the mathematical construction is equivalent to a set of operative axioms that can be used conveniently, in practice, for deciding if a given matrix-sequence is of GLT type and for computing the related symbol. The current formulation is taken from [16, Ch 9], where 9 axioms are listed representing a definition of the GLT class alternative to that in [38,39]. Here, we just give and briefly report and discuss four of these axioms of the GLT class, which are sufficient for our purposes.

Throughout, we use the following notation

$$\{A_n\}_n \sim_{\text{GLT}} \kappa(x, \sigma), \quad \kappa: [0, 1] \times [-\pi, \pi] \rightarrow \mathbb{C},$$

to say that the sequence  $\{A_n\}_n$  is a GLT sequence with GLT symbol  $\kappa(x, \sigma)$ .



Here we list four main features of GLT sequences.

- (1) Let  $\{A_n\}_n \sim_{\text{GLT}} \kappa$  with a function  $\kappa: G \rightarrow \mathbb{C}$ , where  $G$  is the set  $[0, 1] \times [-\pi, \pi]$ , then  $\{A_n\}_n \sim_{\sigma} (\kappa, G)$ . If the matrices  $A_n$  are Hermitian, then it also holds that  $\{A_n\}_n \sim_{\lambda} (\kappa, G)$ .
- (2) The set of GLT sequences forms a  $*$ -algebra, i.e., it is closed under linear combinations, products, conjugation, but also inversion when the symbol is invertible a.e. In formulae, let  $\{A_n\}_n \sim_{\text{GLT}} \kappa_1$  and  $\{B_n\}_n \sim_{\text{GLT}} \kappa_2$ , then

- $\{\alpha A_n + \beta B_n\}_n \sim_{\text{GLT}} \alpha \kappa_1 + \beta \kappa_2, \quad \alpha, \beta \in \mathbb{C};$
- $\{A_n B_n\}_n \sim_{\text{GLT}} \kappa_1 \kappa_2;$
- $\{A_n^*\}_n \sim_{\text{GLT}} \kappa_1^*;$
- $\{A_n^{-1}\}_n \sim_{\text{GLT}} \kappa_1^{-1}$  provided that  $\kappa_1$  is invertible a.e.

- (3) Any sequence of Toeplitz matrices  $\{T_n(f)\}_n$  generated by  $f \in L^1([-\pi, \pi])$  is a GLT matrix-sequence with symbol  $\kappa(x, \sigma) = f(\sigma)$ . For a Riemann integrable function  $a$  defined on  $[0, 1]$ , the corresponding diagonal sampling matrix-sequence

$$\{D_n(a)\}_n$$

is a GLT matrix-sequence with symbol  $\kappa(x, \sigma) = a(x)$  and entries  $[D_n(a)]_{j,j}$  given by  $a(j/n), j = 1, \dots, n$ .

- (4) According to the last part of Definition 1.1, every zero-distributed matrix-sequence is a GLT sequence with symbol 0 and viceversa, i.e.,  $\{A_n\}_n \sim_{\sigma} 0 \iff \{A_n\}_n \sim_{\text{GLT}} 0$ .

Item (1) can be viewed as a generalization of Theorem 1.1 to a much wider, indeed maximal,  $*$ -algebra of matrix-sequences. Items (2) and (3) show that the Toeplitz finite section algebra generated (via adjoints, products, sums, and limits) by all sequences  $\{T_n(f)\}_n$  with continuous symbol (studied e.g. in [19]) and with essentially bounded symbols (studied e.g. in [41]) is contained in the GLT class. The matrix-sequences  $\{D_n(a)\}_n$  are the basic blocks for considering variations along the diagonals, so going outside the Toeplitz setting. The zero-distributed matrix-sequences considered in item (4) contain e.g. as a proper subset any matrix-sequence obtained via finite sections of any given compact operator.

Finally, we stress that the axioms in [16, Ch9] not reported here, essentially contain limit operations via the a.c.s. metric and more eigenvalue distribution results on GLT matrix-sequences, which can be viewed as perturbations of Hermitian GLT matrix-sequences.

If  $f$  is smooth enough, an informal interpretation of the limit relation (1.5) (resp. (1.6)) is that when  $n$  is sufficiently large, then the eigenvalues (resp. singular values) of  $A_n$  can be approximated by a sampling of  $f$  (resp.  $|f|$ ) on a uniform equispaced grid of the domain  $D$ , up to at most few outliers. Often this approximation is good enough: the notion

of GLT momentary symbols has been introduced for obtaining a more accurate approximation of the singular values and, under certain circumstances, also of the eigenvalues. In essence the GLT momentary symbols represent an extension of the GLT theory in which a hierarchy of symbols is present, the first one being the GLT symbol. Taking into account these non-unique hierarchies of symbols (the first one being unique), we can obtain more precise spectral approximations as shown in [12,18].

**Definition 1.2** (GLT momentary symbols). Let  $\{X_n\}_n$  be a matrix-sequence and assume that there exist matrix-sequences  $\{A_n^{(r)}\}_n$ ,  $\{R_n\}_n$ , scalar sequences  $c_n^{(r)}$ ,  $r = 0, \dots, \ell$ , and measurable functions  $f_r$  defined over  $[-\pi, \pi] \times [0, 1]$ ,  $\ell$  nonnegative integer independent of  $n$ , such that  $\{R_n\}_n$  is zero-distributed in accordance with the last part of Definition 1.1,

$$\left\{ \frac{A_n^{(r)}}{c_n^{(r)}} \right\}_n \sim_{\text{GLT}} f_r,$$

$$c_n^{(0)} = 1, \quad c_n^{(s)} = o(c_n^{(r)}), \quad \ell \geq s > r,$$

$$\{X_n\}_n = \{A_n^{(0)}\}_n + \sum_{r=1}^{\ell} \{A_n^{(r)}\}_n + \{R_n\}_n.$$

Then, with a slight abuse of notation

$$f_n = f_0 + \sum_{r=1}^{\ell} c_n^{(r)} f_r$$

is defined as a GLT momentary symbol for  $X_n$  and  $\{f_n\}_n$  is a sequence of GLT momentary symbols for the matrix-sequence  $\{X_n\}_n$ .

Of course, in line with [14,15], the momentary symbols could be matrix-valued with the number of variables equal to  $2d$  and domain  $[-\pi, \pi]^d \times [0, 1]^d$  if the basic matrix-sequences appearing in Definition 1.2 are, up to proper scaling, matrix-valued and multilevel GLT matrix-sequences.

Clearly there is an immediate link with the GLT theory stated in the next result, but many other connections should be investigated; see the proofs in [12,18].

**Theorem 1.2.**  $\{X_n\}_n \sim_{\text{GLT}} f_0$  and  $\lim_{n \rightarrow \infty} f_n = f_0$  uniformly on the definition domain.

Here by making reference to the approximations by Finite Differences, for a fixed positive integer  $\ell$ , we could consider operators of the form

$$\sum_{r=0}^{\ell} (-1)^r \alpha_r \frac{d^{2r}}{dx^{2r}} \tag{1.7}$$

which, by linearity of the approximation technique of the involved operators, and by (1.2), give rise to Toeplitz structures of the type in (1.4) with the expression

$$T_n \left( \sum_{r=0}^{\ell} \alpha_r h^{2(\ell-r)} f_r \right).$$

In perfect analogy, in the case where the approximation is obtained via Isogeometric Analysis, for a fixed positive integer  $\ell$ , we find

$$T_n \left( \sum_{r=0}^{\ell} \alpha_r h^{2(\ell-r)} g_r \right),$$

taking into account (1.3) and again the linearity of the approximation technique and of the considered operators. In both cases it is evident that the related matrix-sequences have  $\sum_{r=0}^{\ell} \alpha_r h^{2(\ell-r)} F_r$  as GLT momentary symbols in the sense of Definition 1.2, with  $F_r$  being either  $f_r$  or  $g_r$ ,  $r = 0, 1, \dots, \ell$ . In both cases we are interested in using the related GLT momentary symbols in terms of a superposition effect for computing the eigenvalues in a fast way

$$\lambda_j \left( T_n \left( \sum_{r=0}^{\ell} \alpha_r h^{2(\ell-r)} F_r \right) \right). \tag{1.8}$$

Notice again that the problem indicated in (1.4) is a special instance of (1.8).

## 2. Main results

For a constant  $\alpha \geq 0$ , the well-known weighted Wiener algebra  $W^\alpha$  is the collection of all functions  $f: [0, 2\pi] \rightarrow \mathbb{C}$ , that can be written as  $f(\sigma) = \sum_{j=-\infty}^{\infty} \mathbf{a}_j(f) e^{i\sigma j}$ , and whose Fourier coefficients  $\mathbf{a}_j(f)$  satisfy

$$\|f\|_\alpha \equiv \sum_{j=-\infty}^{\infty} |\mathbf{a}_j(f)| (|j| + 1)^\alpha < \infty.$$

We address real-valued symbols  $f$  in  $W^\alpha$ , tracing out a simple loop, precisely satisfying the following conditions.

- (i) The range of  $f$  is a segment  $[0, \mu]$  with  $\mu > 0$ .
- (ii)  $f(0) = f(2\pi) = 0$ ,  $f'(0) = f'(2\pi) = 0$ , and  $f''(0) = f''(2\pi) > 0$ .
- (iii) There is a  $\sigma_0 \in (0, 2\pi)$  such that  $f(\sigma_0) = \mu$ ,  $f'(\sigma) > 0$  for  $0 < \sigma < \sigma_0$ ,  $f'(\sigma) < 0$  for  $\sigma_0 < \sigma < 2\pi$ ,  $f'(\sigma_0) = 0$ , and  $f''(\sigma_0) < 0$ .

The collection of all these symbols is called the *simple loop class* and is denoted by  $SL^\alpha$ . In this paper we consider even symbols in  $SL^\alpha$ , that is  $f(s) = f(2\pi - s)$  for each  $s \in [0, \pi]$ . Obviously, it is enough to study such symbols in the interval  $[0, \pi]$ .

For every  $\lambda \in [0, \mu]$  there exists a unique  $s \in [0, \pi]$  satisfying  $f(s) = \lambda$ , and the symbol  $f - \lambda$  has 2 zeros:  $\pm s$ , implying that the Toeplitz operator  $T(f - \lambda)$  is not invertible (see [42, Sc.1]). For  $\alpha \geq 2$  and  $f \in SL^\alpha$ , we define the operator  $B$  as follows

$$\begin{aligned}
 B_f(\sigma, s) &\equiv \frac{f(\sigma) - f(s)}{4 \sin\left(\frac{\sigma-s}{2}\right) \sin\left(\frac{\sigma+s}{2}\right)} \\
 &= \frac{f(\sigma) - f(s)}{2(\cos(s) - \cos(\sigma))} \quad (\sigma \in [0, 2\pi], s \in [0, \pi]).
 \end{aligned}
 \tag{2.1}$$

According to [2], SLM tells us that  $B_f$  is a real-valued and continuous function in  $W^{\alpha-1}$ , which is also bounded away from zero. The resulting operator  $T(B_f(\cdot, s))$  is invertible and therefore, since the finite section method can be applied (see [19] for example), the related finite Toeplitz matrices  $T_n(B_f(\cdot, s))$  are also invertible for every sufficiently large  $n$ . Moreover, since  $B_f$  is bounded away from zero, we can say the same for every  $n > 0$ . Note that  $B_f$  can be thought of as the quotient between  $f - \lambda$  and  $4 \sin((\sigma - s)/2) \sin((\sigma + s)/2)$ , which is similar to the preconditioning process of the ill-conditioned matrix  $T_n(f - \lambda)$  used for example in [43,44]; for a general account on preconditioning in a Toeplitz setting see [16,45] and references therein.

For a function  $u$  with a singularity at some point in the interval  $I$ , let  $\int_I u(x)dx$  be the Cauchy principal value of the singular integral  $\int_I u(x)dx$ . Since the function  $B_f$  belongs to  $W^{\alpha-1}$  and  $B_f(t, s) \neq 0$  for every  $t \in \mathbb{T}$  and every  $s \in [0, \pi]$ , it admits the so called Wiener–Hopf factorization  $B_f = [B_f]_- [B_f]_+$  (index zero) where

$$[B_f]_\pm(t, s) \equiv \exp \left\{ \frac{1}{2} \log B_f(t, s) \pm \frac{1}{2\pi i} \int_{\mathbb{T}} \frac{\log B_f(\tau, s)}{\tau - t} d\tau \right\},$$

$t = e^{i\sigma}$ , and  $\sigma \in [0, 2\pi]$ . The Wiener–Hopf factorization (also called method or decomposition) was introduced by N. Wiener and E. Hopf in 1931. What we call Wiener–Hopf factorization has its origin in the work of Gakhov [46], but Mark Krein [47] was the first to understand the operator theoretic essence and its algebraic background, and to present it in a clear way. For a nice and modern explanation see [48, Ch 1.4].

For  $f \in SL^\alpha$  and  $s \in [0, \pi]$ , we define the operator  $H$  as follows

$$\begin{aligned}
 H_f(s) &\equiv \frac{1}{4\pi} \int_0^{2\pi} \frac{\log B_f(\sigma, s)}{\tan\left(\frac{\sigma-s}{2}\right)} d\sigma - \frac{1}{4\pi} \int_0^{2\pi} \frac{\log B_f(\sigma, s)}{\tan\left(\frac{\sigma+s}{2}\right)} d\sigma \\
 &= \frac{\sin(s)}{2\pi} \int_0^{2\pi} \frac{\log B_f(\sigma, s)}{\cos(s) - \cos(\sigma)} d\sigma.
 \end{aligned}
 \tag{2.2}$$

The function  $H_f$  can be understood as the continuous argument of the map

$$s \mapsto \frac{[B_f]_+(e^{is}, s)[B_f]_-(e^{-is}, s)}{[B_f]_+(e^{-is}, s)[B_f]_-(e^{is}, s)},$$

playing a key role in SLM.

SLM tells us, in particular, that the eigenvalues of  $T_n(f)$  are given by

$$\lambda_j(T_n(f)) = f(\sigma_{j,n}) + \sum_{\ell=1}^{[\alpha]} c_\ell(\sigma_{j,n}) h^\ell + E(\sigma_{j,n}), \tag{2.3}$$

where

- the eigenvalues of  $T_n(f)$  are arranged in nondecreasing order;
- $h \equiv 1/(n + 1)$  and  $\sigma_{j,n} \equiv \pi j h$ ;
- the coefficients  $c_\ell$  depend only on  $f$  and can be found explicitly, for example

$$c_1 = -f' H_f, \quad c_2 = \frac{1}{2} f'' H_f^2 + f' H_f H'_f; \tag{2.4}$$

- $E(\sigma_{j,n}) = O(h^\alpha)$  is the remainder (error) term, which satisfies the inequality  $|E(\sigma_{j,n})| \leq \kappa h^\alpha$  for some constant  $\kappa$  depending only on  $f$ .

For  $f, g \in \text{SL}^\alpha$  and a constant  $\beta \in \mathbb{R}_+$ , we now investigate the relationship between the eigenvalues  $\lambda_j(T_n(f))$ ,  $\lambda_j(T_n(g))$ , and  $\lambda_j(T_n(f + \beta g))$ . From (2.3) we easily obtain

$$\lambda_j(T_n(f + \beta g)) = f(\sigma_{j,n}) + \beta g(\sigma_{j,n}) + O(h).$$

Indeed, as a challenge in the field, we are looking for a more detailed result involving a complete expansion and a real positive constant  $\beta_n$  depending on  $n$ . The (momentary) symbol  $f + \beta_n g$  depends on  $n$ , and as a consequence SLM cannot be applied. However, under proper adjustments, the quoted technique can be used when  $\beta_n$  is  $h$  or  $h^h$ , see Theorems 2.2 and 2.3.

**Remark 2.1.** The condition  $\beta_n \rightarrow 0$  as  $n \rightarrow \infty$  can be implemented in both cases by simply writing

$$f + h^h g = f + g + (h^h - 1)g,$$

and noticing that  $h^h - 1 \rightarrow 0$  as  $n \rightarrow \infty$ . Moreover, we believe that our results can be extended to any symbol with the form  $f_0 + \beta_{n,1} f_1 + \dots + \beta_{n,\ell} f_\ell$ , where  $f_0 \in \text{SL}^\alpha$  with  $\alpha \geq 2$ , for every  $k = 1, \dots, \ell$ ,  $f_k$  is a differentiable function with  $f'_k(0) = f'_k(\pi)$ ,  $\beta_{n,k} \rightarrow 0$  as  $n \rightarrow \infty$ , and  $n$  is sufficiently large. It will be the topic of a future investigation.

We start with the symbol  $f + hg$ , that is  $\beta_n = h$ . Consider the function

$$\psi(s) \equiv \frac{\sin(s)}{2\pi} \int_0^{2\pi} \frac{B_g(\sigma, s)}{B_f(\sigma, s)(\cos(s) - \cos(\sigma))} d\sigma.$$

**Theorem 2.2.** *Let  $f$  and  $g$  be two even symbols in  $SL^\alpha$  with  $\alpha \geq 2$ . Then*

$$\lambda_j(T_n(f + gh)) = f(\sigma_{j,n}) + \sum_{\ell=1}^{[\alpha]} \mathfrak{r}_\ell(\sigma_{j,n})h^\ell + E(\sigma_{j,n}),$$

where  $\mathfrak{r}_\ell$  are bounded functions from  $[0, \pi]$  to  $\mathbb{R}$  depending only on  $f, g$  that can be explicitly determined. For instance

$$\begin{aligned} \mathfrak{r}_1 &= g - f'H_f, \\ \mathfrak{r}_2 &= \frac{1}{2}f''H_f^2 + f'H_fH'_f - f'\psi - g'H_f. \end{aligned}$$

The remainder  $E(\sigma_{j,n}) = O(h^\alpha)$  satisfies the inequality  $|E(\sigma_{j,n})| \leq \kappa h^\alpha$  for some constant  $\kappa$  depending only on  $f$  and  $g$ .

For the next result we will study the eigenvalues corresponding to the symbol  $f + h^h g$ , that is  $\beta_n = h^h$ . Consider the function

$$\varphi(s) \equiv \frac{\sin(s)}{2\pi} \int_0^{2\pi} \frac{B_g(\sigma, s)}{(B_f(\sigma, s) + B_g(\sigma, s))(\cos(s) - \cos(\sigma))} d\sigma.$$

**Theorem 2.3.** *Let  $f$  and  $g$  be two even symbols in  $SL^\alpha$  with  $\alpha \geq 2$ . Then*

$$\lambda_j(T_n(f + h^h g)) = f(\sigma_{j,n}) + g(\sigma_{j,n}) + \sum_{\ell=1}^{[\alpha]} \sum_{k=0}^{\ell} \mathfrak{s}_{\ell,k}(\sigma_{j,n})h^\ell \log^k(h) + \hat{E}(\sigma_{j,n}),$$

where  $\mathfrak{s}_{\ell,k}$  are bounded functions from  $[0, \pi]$  to  $\mathbb{R}$  depending only on  $f, g$  that can be explicitly determined. For instance

$$\begin{aligned} \mathfrak{s}_{1,1} &= g, \\ \mathfrak{s}_{1,0} &= -H_{f+g}(f' + g'), \\ \mathfrak{s}_{2,2} &= \frac{1}{2}g, \\ \mathfrak{s}_{2,1} &= -\varphi(f' + g') - g'H_{f+g}, \\ \mathfrak{s}_{2,0} &= \frac{1}{2}H_{f+g}^2(f'' + g'') + H_{f+g}H'_{f+g}(f' + g'). \end{aligned}$$

The term  $\hat{E}(\sigma_{j,n}) = O(h^\alpha |\log^\alpha(h)|)$  plays the role of a remainder or error and satisfies the inequality  $|\hat{E}(\sigma_{j,n})| \leq \kappa h^\alpha |\log^\alpha(h)|$  for some constant  $\kappa$  depending only on  $f$  and  $g$ .

### 3. Proof of the main results

Let  $\chi_m(t) \equiv t^m$  and consider the polynomial

$$\Theta_k(t, s) = [T_k^{-1}(B_f(\cdot, s))\chi_0](t).$$

The following theorem contains the SLM results which are relevant to the present work. The proofs can be found in [2].

**Theorem 3.1.** *Let  $h = 1/(n + 1)$ ,  $\alpha \geq 2$  and  $u$  be an even function in  $\in \text{SL}^\alpha$ .*

- (i)  $B_u(\cdot, s)$  belongs to  $W^{\alpha-1}$  uniformly in  $s \in [0, \pi]$ , is real-valued, positive, bounded, and bounded away from zero.
- (ii)  $B_u(\cdot, s)$  admits a Wiener–Hopf factorization with index zero, moreover the factors  $[B_u(\cdot, s)]_{\pm}^{\pm 1}$  belong to  $W_{\pm}^{\alpha-1}$  uniformly in  $s \in [0, \pi]$ , where  $W_{\pm}^{\alpha-1}$  are the subalgebras of  $W^{\alpha-1}$  given by

$$W_{\pm}^{\alpha-1} \equiv \left\{ u(t) = \sum_{j=0}^{\infty} \mathbf{a}_{\pm j}(u) t^{\pm j} : \|u\|_{\alpha-1} < \infty \right\}.$$

- (iii) The number  $\lambda = f(s)$  is an eigenvalue of  $T_n(u)$  if and only if

$$e^{-2i(n+1)s} \Theta_{n+2}(e^{is}, s) \overline{\Theta_{n+2}(e^{-is}, s)} = \Theta_{n+2}(e^{-is}, s) \overline{\Theta_{n+2}(e^{is}, s)}. \tag{3.1}$$

Our specific aim is to recreate SLM working with the momentary symbol  $f + \beta_n g$  for two particular values of  $\beta_n$ . Suppose that  $\alpha \geq 2$ ,  $f, g \in \text{SL}^\alpha$ , and take  $\beta_n = h$  or  $\beta_n = h^h$ . If  $f$  and  $g$  are even, the function  $f + \beta_n g$  belongs to  $\text{SL}^\alpha$ . Then the results in Theorem 3.1 can be applied to  $u = f + \beta_n g$ . From (2.1) we easily get  $B_{f+\beta_n g} = B_f + \beta_n B_g$ . Moreover, the polynomial  $\Theta_k$  becomes

$$\Theta_k(t, s) = [\{T_k(B_f(\cdot, s)) + \beta_n T_k(B_g(\cdot, s))\}^{-1} \chi_0](t). \tag{3.2}$$

Then part (iii) of Theorem 3.1 tells us that the number  $\lambda = f(s) + \beta_n g(s)$  is an eigenvalue of  $T_n(f + \beta_n g)$  if and only if (3.1) is true. This an exact implicit equation for the eigenvalues of  $T_n(f + \beta_n g)$  and the theoretical base for our individual asymptotic expansions.

We now find an expansion for the polynomial  $\Theta_n$  in terms of  $B_f$  and  $B_g$ . Suppose that  $u(t) = \sum_{j=-\infty}^{\infty} u_j t^j$  ( $t \in \mathbb{T}$ ) belongs to  $L^2(\mathbb{T})$  and recall the usual operators

$$[P_n u](t) \equiv \sum_{j=0}^{n-1} u_j t^j, \quad [Q_n u](t) \equiv \sum_{j=n}^{\infty} u_j t^j, \quad [Pu](t) \equiv \sum_{j=0}^{\infty} u_j t^j.$$

For  $u \in L^\infty(\mathbb{T})$ , it is well-known that the Toeplitz operator  $T(u): L^2(\mathbb{T}) \rightarrow L^2(\mathbb{T})$  is defined as  $T(u) \equiv PuP$  while the (finite) Toeplitz matrix  $T_n(u)$  coincides with  $P_n u P_n$ .

**Lemma 3.2.** *For  $\alpha \geq 2$ , let  $f, g$  be even functions in  $SL^\alpha$ . Take  $\beta_n$  as  $h$  or  $h^h$ . Then we have*

$$\Theta_n(t, s) = [B_f + \beta_n B_g]_{+}^{-1}(t, s) + R_n(t, s),$$

where  $\sup\{|R_n(t, s)|: (t, s) \in \mathbb{T} \times [0, \pi]\} = o(h^{\alpha-1})$  as  $n \rightarrow \infty$ .

**Proof.** Let  $\beta_n$  be  $h$  or  $h^h$ . From part (i) of Theorem 3.1 with  $u = f + \beta_n g$ , we know that for every  $s \in [0, \pi]$ ,  $B_{f+\beta_n g}(\cdot, s) = B_f(\cdot, s) + \beta_n B_g(\cdot, s)$  is positive and bounded away from zero, hence the matrix  $T_n(B_f(\cdot, s))$  is invertible for every  $n \geq 1$ , uniformly in  $s \in [0, \pi]$ .

According to [48, p. 10], for a function  $a \in L^\infty(\mathbb{T})$ , the inverse of the operator  $T(a)$  is  $T^{-1}(a) = [B_a]_{+}^{-1}(\cdot, s)P[B_a]_{-}^{-1}(\cdot, s)$ . To simplify the notation, in this proof write  $B(t, s)$  instead of  $B_{f+\beta_n g}(t, s)$ . Then, the relation

$$T^{-1}(B(\cdot, s))\chi_0 = B_{+}^{-1}(\cdot, s)PB_{-}^{-1}(\cdot, s)\chi_0 = B_{+}^{-1}(\cdot, s),$$

is a consequence of  $PB_{-}(t, s) = B_{-}(\infty, s) = 1$  and  $PB_{-}^{-1}(t, s) = B_{-}^{-1}(\infty, s) = 1$ , where, by part (ii) of Theorem 3.1, the Wiener–Hopf factors  $B_{\pm}^{-1}$  belong to  $W_{\pm}^{\alpha-1}$  uniformly in  $s \in [0, \pi]$ .

From (3.2) we obtain

$$\begin{aligned} \Theta_n(t, s) &= [T_n^{-1}(B(\cdot, s))\chi_0](t) \\ &= [T^{-1}(B(\cdot, s))\chi_0](t) + \{[T_n^{-1}(B(\cdot, s)) - T^{-1}(B(\cdot, s))]\chi_0\}(t) \\ &= B_{+}^{-1}(t, s) + R_n(t, s), \end{aligned}$$

where  $R_n(t, s) = \{[T_n^{-1}(B(\cdot, s)) - T^{-1}(B(\cdot, s))]\chi_0\}(t)$ . Since  $P_n$  converges strongly to  $P$ ,  $T_n$  converges strongly to  $T$ , and hence  $R_n$  is expected to be “small” as  $n \rightarrow \infty$ . Omitting the argument  $(\cdot, s)$  the calculation continues as follows,

$$\begin{aligned} R_n &= T_n^{-1}(B)\{T(B) - T_n(B)\}T^{-1}(B)\chi_0 - Q_n T^{-1}(B)\chi_0 \\ &= T_n^{-1}(B)\{PBP - P_n B P_n\}B_{+}^{-1}PB_{-}^{-1}\chi_0 - Q_n B_{+}^{-1}PB_{-}^{-1}\chi_0, \end{aligned}$$

which by the identities  $PBP = P_n B P_n + P_n B Q_n + Q_n B P$  and  $Q_n B B_{+}^{-1} = Q_n B_{-} = 0$ , becomes



$$R_n = T_n^{-1}(B)P_nBQ_nB_+^{-1} - Q_nB_+^{-1}.$$

To find a bound for the norm of  $T_n^{-1}(B) = T_n^{-1}(B_{f+\beta_n g}(\cdot, s))$ , as  $n \rightarrow \infty$ , we note that its operator norm in the Wiener algebra  $W^{\alpha-1}$  equals its largest eigenvalue (which must be real and positive) times a positive constant, and which is naturally bounded by  $\inf\{B_{f+\beta_n g}(s) : 0 \leq s \leq \pi\}^{-1}$ . Then there exists a positive constant  $k$  such that

$$\|T_n^{-1}(B_{f+\beta_n g}(\cdot, s))\|_{\alpha-1} \leq k \inf\{B_f(s) + \beta_n B_g(s) : 0 \leq s \leq \pi\}^{-1}.$$

If  $\beta_n$  takes the value  $h$ , the last infimum is greater than  $\inf\{B_f(s) : 0 \leq s \leq \pi\}$ , while if  $\beta_n = h^h$  it is greater than

$$\inf\{B_f(s) : 0 \leq s \leq \pi\} + \inf\{B_g(s) : 0 \leq s \leq \pi\}.$$

In both cases the provided bound is positive, finite, and independent of  $n$ , that is  $\|T_n^{-1}(B)\|_{\alpha-1} \leq \kappa$  for some  $\kappa > 0$ .

Using the inequalities  $\|\cdot\|_{L^\infty} \leq \|\cdot\|_0 \leq \|\cdot\|_{\alpha-1}$  and

$$\|Q_n a\|_0 \leq \sum_{j=n}^{\infty} |a_j(a)|(1+j)^{\alpha-1} h^{\alpha-1} = \|Q_n a\|_{\alpha-1} h^{\alpha-1} = o(h^{\alpha-1}),$$

as  $n \rightarrow \infty$ , we reach

$$\begin{aligned} \|R_n\|_{L^\infty} &\leq \|R_n\|_0 \\ &\leq \|T_n^{-1}(B)P_nBQ_nB_+^{-1}\|_0 + \|Q_nB_+^{-1}\|_0 \\ &= \|T_n^{-1}(B)\|_0\{\|P_nB\|_0 + 1\}\|Q_nB_+^{-1}\|_0 \\ &\leq \kappa\{\|P_nB\|_{\alpha-1} + 1\}o(h^{\alpha-1}) = o(h^{\alpha-1}), \end{aligned}$$

uniformly in  $s \in [0, \pi]$ , completing the proof.  $\square$

The following theorem is a consequence of Theorem 3.1 and Lemma 3.2. Since the proof can be found in [2] we present it here without a proof.

**Theorem 3.3.** *Let  $h = 1/(n + 1)$ ,  $\alpha \geq 2$  and  $u$  be an even function in  $\in \text{SL}^\alpha$ .*

- (i) *For every sufficiently large natural number  $n$  there exists a real-valued function  $\hat{R}_n \in C[0, \pi]$  such that a number  $\lambda = u(s)$  is an eigenvalue of  $T_n(u)$  if and only if*

$$(n + 1)s + H_u(s) - \hat{R}_n(s) = j\pi, \tag{3.3}$$

*for some  $j \in \mathbb{Z}$ , and  $\hat{R}_n(0) = \hat{R}_n(\pi) = 0$ ,  $\sup\{|\hat{R}_n(s)| : s \in [0, \pi]\} = o(h^{\alpha-1})$  as  $n \rightarrow \infty$ .*

- (ii) For every sufficiently large  $n$  there exists pairwise disjoint intervals  $I_{j,n}$  ( $j = 1, \dots, n$ ) such that (3.3) and its truncated version

$$(n + 1)s + H_u(s) = j\pi,$$

have unique solutions  $s_{j,n}$  and  $\hat{s}_{j,n}$  in  $I_{j,n}$ , respectively, for every  $j = 1, \dots, n$ . Moreover,  $|s_{j,n} - \hat{s}_{j,n}| = o(h^\alpha)$ .

- (iii) For each  $j = 1, \dots, n$ , the function

$$\Phi_{j,n}(s) \equiv \sigma_{j,n} - H_u(s)h,$$

is a contraction on  $[0, \pi]$ , and the sequence defined by

$$\hat{s}_{j,n}^{(0)} \equiv \sigma_{j,n} \quad \text{and} \quad \hat{s}_{j,n}^{(\ell)} \equiv \Phi_{j,n}(\hat{s}_{j,n}^{(\ell-1)}), \quad \ell \geq 1,$$

satisfies  $|\hat{s}_{j,n} - \hat{s}_{j,n}^{(\ell)}| = O(h^{\ell+1})$ .

It is clear that  $B_{f+\beta ng} = B_f + \beta_n B_g$  but the situation with  $H$  is more delicate. Hence we decided to expand  $H_{f+\beta ng}$  into factors with coefficients not involving  $n$ . We continue with the following technical result.

**Lemma 3.4.** For  $\alpha \geq 2$ , let  $f, g$  be even functions in  $SL^\alpha$ . As  $n \rightarrow \infty$ , we have

- (i)  $H_{f+hg}(s) = H_f(s) + \psi(s)h + O(h^2)$ ,
- (ii)  $H_{f+h^h g}(s) = H_{f+g}(s) + \varphi(s)h \log(h) + O(h^2 \log^2(h))$ ,

where  $\psi, \varphi$  are  $\lfloor \alpha \rfloor - 1$  times continuously differentiable functions, given by

$$\psi(s) \equiv \frac{\sin(s)}{2\pi} \int_0^{2\pi} \frac{B_g(\sigma, s)}{B_f(\sigma, s)(\cos(s) - \cos(\sigma))} d\sigma,$$

$$\varphi(s) \equiv \frac{\sin(s)}{2\pi} \int_0^{2\pi} \frac{B_g(\sigma, s)}{(B_f(\sigma, s) - B_g(\sigma, s))(\cos(s) - \cos(\sigma))} d\sigma.$$

**Proof.** From part (i) of Theorem 3.1 we know that  $s \mapsto B_f(\cdot, s)$  and  $s \mapsto B_g(\cdot, s)$  act continuously from  $[0, \pi]$  to  $W^{\alpha-1}$ , which combined with the fact that the singular integral operator is continuous over the weighted Wiener algebra  $W^{\alpha-1}$ , implies that  $\psi, \varphi$  are  $\lfloor \alpha \rfloor - 1$  times continuously differentiable functions. For the part (i), we use the expansion

$$\begin{aligned} \log(B_f + hB_g) &= \log(B_f) + \log\left(1 + \frac{B_g}{B_f}h\right) \\ &= \log(B_f) + \frac{B_g}{B_f}h - \frac{B_g^2}{2B_f^2}h^2 + O(h^3). \end{aligned}$$

Then, the function  $H_f$  in (2.2) becomes

$$\begin{aligned} H_{f+hg}(s) - H_f(s) &= \frac{\sin(s)}{2\pi} \int_0^{2\pi} \frac{\log(B_f(\sigma, s) + B_g(\sigma, s)h) - \log B_f(\sigma, s)}{\cos(s) - \cos(\sigma)} d\sigma \\ &= \psi(s)h + O(h^2), \end{aligned}$$

proving the first part.

For the part (ii), as  $n \rightarrow \infty$ , we use the expansion

$$h^h = e^{h \log(h)} = 1 + h \log(h) + \frac{1}{2}h^2 \log^2(h) + O(h^3 |\log^3(h)|)$$

and we easily arrive at

$$B_f + h^h B_g = B_f + B_g + h \log(h) B_g + \frac{1}{2}h^2 \log^2(h) B_g + O(h^3 |\log^3(h)|).$$

Note that for every  $n$  the functions  $B_f + h^h B_g$  and  $B_f + B_g$  are positive, bounded, and bounded away from zero. Thus we can apply the logarithm to the former and expand around the latter, obtaining

$$\begin{aligned} \log(B_f + h^h B_g) &= \log(B_f + B_g) + \frac{B_g}{B_f + B_g} h \log(h) \\ &\quad + \frac{B_f B_g}{2(B_f + B_g)} h^2 \log^2(h) + O(h^3 |\log^3(h)|). \end{aligned}$$

Finally, the second part is a direct consequence of the last expression in combination with (2.2).  $\square$

**Proof of Theorem 2.2.** Assume that  $2 \leq \alpha < 3$  and let  $\beta_n = h$ , and for simplicity write  $\sigma$  instead of  $\sigma_{j,n}$ . Taking  $u = f + hg$  and combining Lemmas 3.2 and 3.4, and part (i) of Theorem 3.3, we infer

$$G_n(s) = j\pi, \tag{3.4}$$

where  $G_n(s) \equiv (n + 1)s + H_f(s) + \psi(s)h - \hat{R}_n(s)$ . The function  $G_n$  is continuous on the interval  $[0, \pi]$  with  $G_n(0) = 0$  and  $G_n(\pi) = \pi(n + 1)$ . By the Intermediate Value Theorem, for each  $j \in \{1, \dots, n\}$  (3.4) has at least one solution in  $(0, \pi)$ . The uniqueness is given by part (ii) of Theorem 3.3 and its denoted by  $s_{j,n}$ . Hence we know that

(i) the eigenvalues of  $T_n(f + hg)$  are all distinct:

$$\lambda_1(T_n(f + hg)) < \dots < \lambda_n(T_n(f + hg));$$

- (ii) the numbers  $s_{j,n}$  given by  $[f + hg](s_{j,n}) = \lambda_j(T_n(f + hg))$  for  $j = 1, \dots, n$ , satisfy the relation (3.4) with  $\hat{R}_n(s_{j,n}) = o(h^{\alpha-1})$  as  $n \rightarrow \infty$ , uniformly in  $j$ .

Let  $F_n(s) \equiv (n + 1)s + H_f(s) + \psi(s)h$ . Hence, by parts (ii) and (iii) of Theorem 3.3 with  $u = f + hg$  we know that  $F_n(s) = \pi j$  has a unique solution  $\hat{s}_{j,n}$  for each  $j = 1, \dots, n$ , satisfying the inequality  $|s_{j,n} - \hat{s}_{j,n}| = o(h^\alpha)$ , and that the function

$$\Phi_{j,n}(s) \equiv \sigma - H_f(s)h - \psi(s)h^2,$$

is a contraction on  $[0, \pi]$ . In addition, the sequence defined by

$$\hat{s}_{j,n}^{(0)} \equiv \sigma \quad \text{and} \quad \hat{s}_{j,n}^{(\ell)} \equiv \Phi_{j,n}(\hat{s}_{j,n}^{(\ell-1)}) \quad (\ell \geq 1),$$

satisfies  $|\hat{s}_{j,n} - \hat{s}_{j,n}^{(\ell)}| = O(h^{\ell+1})$ .

Write (3.4) as  $s = \Phi_{j,n}(s) + \Delta_n(s)$  where  $\Delta_n(s) = o(h^\alpha) + O(h^3)$  as  $n$  grows to infinity. We will iterate over the relation  $s = \Phi_{j,n}(s)$ . We have  $\hat{s}_{j,n}^{(0)} = \sigma$  and  $\hat{s}_{j,n}^{(1)} = \Phi_{j,n}(\hat{s}_{j,n}^{(0)}) = \sigma - H_f(\sigma)h - \psi(\sigma)h^2$ . To evaluate  $\hat{s}_{j,n}^{(2)}$  first note that

$$\begin{aligned} H_f(\hat{s}_{j,n}^{(1)}) &= H_f(\sigma) - H'_f(\sigma)\{H_f(\sigma)h + \psi(\sigma)h^2\} \\ &\quad + \frac{1}{2}H''_f(\sigma)\{H_f^2(\sigma) + \psi^2(\sigma)h^2 + 2H_f(\sigma)\psi(\sigma)h\}h^2 + O(h^3) \\ &= H_f(\sigma) - H_f(\sigma)H'_f(\sigma)h + \left\{ \frac{1}{2}H_f^2(\sigma)H''_f(\sigma) - H'_f(\sigma)\psi(\sigma) \right\}h^2 + O(h^3), \end{aligned}$$

and that

$$\begin{aligned} \psi(\hat{s}_{j,n}^{(1)}) &= \psi(\sigma) - \psi'(\sigma)\{H_f(\sigma)h + \psi(\sigma)h^2\} \\ &\quad + \frac{1}{2}\psi''(\sigma)\{H_f^2(\sigma) + \psi^2(\sigma)h^2 + 2H_f(\sigma)\psi(\sigma)h\}h^2 + O(h^3) \\ &= \psi(\sigma) - \psi'(\sigma)H_f(\sigma)h + O(h^2). \end{aligned}$$

Now by the Taylor theorem we obtain

$$\begin{aligned} \hat{s}_{j,n}^{(2)} &= \sigma - H_f(\sigma - H_f(\sigma)h - \psi(\sigma)h^2)h - \psi(\sigma - H_f(\sigma)h - \psi(\sigma)h)h^2 \\ &= \sigma - H_f(\sigma)h + \{H_f(\sigma)H'_f(\sigma) - \psi(\sigma)\}h^2 + O(h^3), \end{aligned}$$

which combined with  $|s_{j,n} - \hat{s}_{j,n}^{(2)}| = o(h^\alpha) + O(h^3)$  proves the theorem for the case  $2 \leq \alpha < 3$ . The remaining cases can be proved, essentially in the same manner.  $\square$

**Proof of Theorem 2.3.** Taking  $\beta_n = h^h$ , mimicking the proof of Theorem 2.2 we obtain

$$\begin{aligned} G_n(s) &\equiv (n + 1)s + H_{f+g}(s) + \varphi(s)h \log(h), \\ F_n(s) &\equiv (n + 1)s + H_{f+g}(s) + \varphi(s)h \log(h), \\ \Phi_{j,n}(s) &\equiv \sigma - H_{f+g}(s)h - \varphi(s)h^2 \log(h). \end{aligned}$$

The remainder function  $\Delta_n$  now has order  $o(h^\alpha) + O(h^3 \log^2(h))$  as  $n \rightarrow \infty$ ,  $\hat{s}_{j,n}^{(0)} = \sigma$ , and  $\hat{s}_{j,n}^{(1)} = \Phi_{j,n}(\hat{s}_{j,n}^{(0)}) = \sigma - H_{f+g}(\sigma)h - \varphi(\sigma)h^2 \log(h)$ . To evaluate  $\hat{s}_{j,n}^{(2)}$  first note that

$$\begin{aligned} H_{f+g}(\hat{s}_{j,n}^{(1)}) &= H_{f+g}(\sigma) - H'_{f+g}(\sigma)\{H_{f+g}(\sigma)h + \varphi(\sigma)h^2 \log(h)\} \\ &\quad + \frac{1}{2}H''_{f+g}(\sigma)\{H^2_{f+g}(\sigma) + \varphi^2(\sigma)h^2 \log^2(h) \\ &\quad + 2H_{f+g}(\sigma)\varphi(\sigma)h \log(h)\}h^2 + O(h^3 |\log^3(h)|) \\ &= H_{f+g}(\sigma) - H_{f+g}(\sigma)H'_{f+g}(\sigma)h \\ &\quad + \left\{ \frac{1}{2}H^2_{f+g}(\sigma)H''_{f+g}(\sigma) - H'_{f+g}(\sigma)\varphi(\sigma) \log(h) \right\}h^2 + O(h^3 |\log^3(h)|), \end{aligned}$$

and that

$$\begin{aligned} \varphi(\hat{s}_{j,n}^{(1)}) &= \varphi(\sigma) - \varphi'(\sigma)\{H_{f+g}(\sigma)h + \varphi(\sigma)h^2 \log(h)\} \\ &\quad + \frac{1}{2}\varphi''(\sigma)\{H^2_{f+g}(\sigma) + \varphi^2(\sigma)h^2 \log^2(h) + 2H_{f+g}(\sigma)\varphi(\sigma)h \log(h)\}h^2 \\ &\quad + O(h^3 |\log^3(h)|) \\ &= \varphi(\sigma) - \varphi'(\sigma)H_{f+g}(\sigma)h + O(h^2 |\log(h)|). \end{aligned}$$

Now by the Taylor theorem we obtain

$$\hat{s}_{j,n}^{(2)} = \sigma - H_{f+g}(\sigma)h + \{H_{f+g}(\sigma)H'_{f+g}(\sigma) - \varphi(\sigma) \log(h)\}h^2 + O(h^3 |\log^3(h)|),$$

which combined with  $|s_{j,n} - \hat{s}_{j,n}^{(2)}| = o(h^\alpha) + O(h^3 |\log^3(h)|)$  give us the theorem for the case  $2 \leq \alpha < 3$ . The remaining cases can be readily proved.  $\square$

#### 4. Numerical tests and an algorithm proposal

The purpose of our main results is to provide asymptotic expansions revealing the fine structure of the eigenvalue behavior in a matrix-less fashion, that is, without the need of any matrix inversion, multiplication by vectors, or even the storage of its entries. Such an expansion has proved to be useful in several applications. In [3,4] the authors exploited those expansions and provided a clever and fully numerical algorithm that calculates the eigenvalues of arbitrarily large matrices within machine precision. More

specifically they devised an extrapolation algorithm for computing the eigenvalues of banded symmetric Toeplitz matrices with a high level of accuracy and low computation cost, starting from the computation of the eigenvalues of small size matrices, in the same spirit of the classical extrapolation procedures for the summation of smooth functions.

As in previous works, the purpose of this section is to show the performance of our asymptotic expansions and to prove that they deliver good approximations even for values of  $n$  in the early hundreds. The numerical calculation of the involved singular integrals is very difficult, therefore we opted to use a standard regularization trick (see [1, Ch 7]), which works as follows. For an integral of the form

$$I(v) = \int_{\gamma}^{\delta} \frac{\mathfrak{f}(u, v)}{\mathfrak{h}(u, v)} du,$$

where for some  $u_0 \in [\gamma, \delta]$ , we have  $\mathfrak{h}(u_0, v) = 0$  and  $\mathfrak{f}(u_0, v) \neq 0$ . We can write

$$I(v) = \int_{\gamma}^{\delta} \frac{\mathfrak{f}(u, v) - \mathfrak{f}(u_0, v)}{\mathfrak{h}(u, v)} du + \mathfrak{f}(u_0, v) \int_{\gamma}^{\delta} \frac{du}{\mathfrak{h}(u, v)},$$

and in most cases, the above integrals are easier to tackle than  $I$  itself. For the case of  $H_f$ , the value of  $\int_0^{2\pi} \cot\left(\frac{\sigma-s}{2}\right) d\sigma$  is 0, and hence we obtain

$$H_f(s) = \frac{\sin(s)}{2\pi} \int_0^{2\pi} \frac{\log B_f(\sigma, s) - \log B_f(s, s)}{\cos(s) - \cos(\sigma)} d\sigma,$$

where  $B_f(s, s)$  can be calculated with the L'Hôpital rule as

$$B_f(s, s) = \frac{f'(s)}{2\sin(s)}, \quad B_f(0, 0) = \frac{f''(0)}{2}, \quad \text{and} \quad B_f(\pi, \pi) = -\frac{f''(0)}{2}.$$

Let  $f$  be a generating function and let  $\lambda_j^{\text{SL}(k)}(T_n(f))$  be the  $k$ th term approximation of  $\lambda_j(T_n(f))$  given by our Theorems 2.2 and 2.3. For the numerical experiments, we consider the individual error

$$E_{j,n}^{\text{SL}(k)} \equiv \lambda_j(T_n(f)) - \lambda_j^{\text{SL}(k)}(T_n(f)),$$

and the corresponding individual and maximal absolute errors

$$AE_{j,n}^{\text{SL}(k)} \equiv |E_{j,n}^{\text{SL}(k)}|, \quad AE_n^{\text{SL}(k)} \equiv \max\{|E_{j,n}^{\text{SL}(k)}| : j = 1, \dots, n\}.$$

We introduce also the individual relative errors

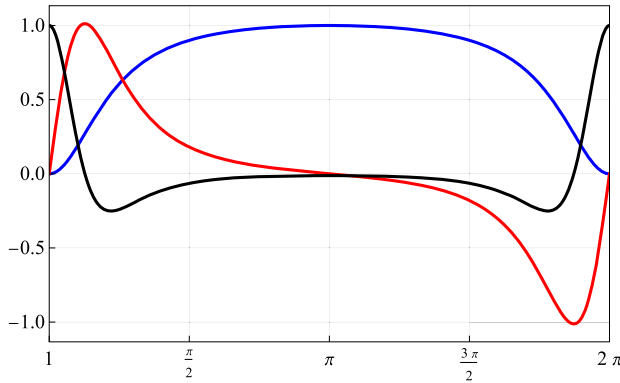


Fig. 1. The generating function  $f(\sigma) = \frac{(1+\rho)^2}{2} \cdot \frac{1-\cos(\sigma)}{1-2\rho\cos(\sigma)+\rho^2}$ , see (4.1), and its first two derivatives for  $\rho = 1/2$ . The blue, red, and black curves are  $f/\|f\|_\infty$ ,  $f'/\|f'\|_\infty$ , and  $f''/\|f''\|_\infty$ , respectively. (For interpretation of the colors in the figure(s), the reader is referred to the web version of this article.)

$$RE_{j,n}^{SL(k)} \equiv \frac{|\lambda_j(T_n(f)) - \lambda_j^{SL(k)}(T_n(f))|}{|\lambda_j(T_n(f))|} = \frac{AE_{j,n}^{SL(k)}}{|\lambda_j(T_n(f))|},$$

which are useful when measuring the approximation of “small” eigenvalues.

#### 4.1. The simple-loop case

For a constant  $0 < \rho < 1$ , consider the simple-loop function given by

$$f(\sigma) \equiv \frac{(1 + \rho)^2}{2} \cdot \frac{1 - \cos(\sigma)}{1 - 2\rho \cos(\sigma) + \rho^2} \quad (0 \leq \sigma \leq 2\pi). \tag{4.1}$$

The respective Fourier coefficients can be exactly calculated as  $\mathbf{a}_k(f) = \frac{1}{4}(\rho^2 - 1)\rho^{|k|-1}$  for  $k \neq 0$  and  $\frac{1}{2}(1 + \rho)$  for  $k = 0$ . This symbol was inspired in the Kac–Murdock–Szegő Toeplitz matrices introduced in [49] and subsequently studied in [50,51], which are usually present in important physics models. We have

$$\|f\|_\alpha = \frac{1 + \rho}{2} + \frac{\rho^2 - 1}{2\rho} \sum_{k=1}^\infty \rho^k (k + 1)^\alpha,$$

which is finite for every  $\alpha > 0$ , the remaining simple-loop conditions are easily verified (see Fig. 1). Then  $f \in SL^\alpha$  for any  $\alpha > 0$ .

In this case it is possible to deduce elementary expressions for the factors of the Wiener–Hopf factorization of  $B_f$ , indeed

$$[B_f]_+(t, s) = \frac{(1 - \rho^2)^2}{4(1 - \rho t)(1 - 2\rho \cos(s) + \rho^2)}, \quad [B_f]_-(t, s) = \frac{1}{1 - \rho t^{-1}}.$$

The function  $H_f$  from (2.2) is therefore nicely given by

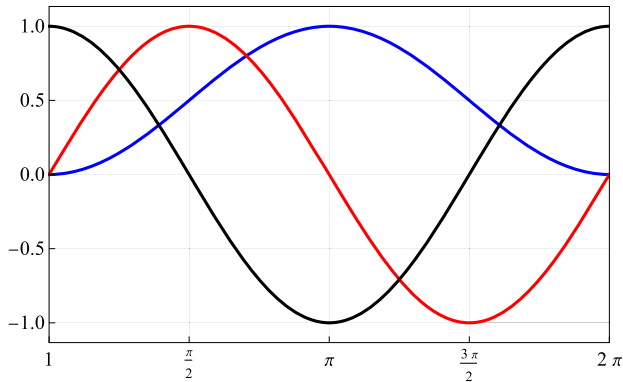


Fig. 2. The generating function  $g(\sigma) = 4 \sin^2(\frac{\sigma}{2})$ , see (4.2), and its first two derivatives. The blue, red, and black curves are  $g/\|g\|_\infty$ ,  $g'/\|g'\|_\infty$ , and  $g''/\|g''\|_\infty$ , respectively.

$$H_f(s) = 2 \arctan\left(\frac{\rho \sin(s)}{1 - \rho \cos(s)}\right).$$

Our second simple-loop function is given by

$$g(\sigma) \equiv 4 \sin^2\left(\frac{\sigma}{2}\right) = 2 - 2 \cos(\sigma). \tag{4.2}$$

The respective Fourier coefficients can be calculated as  $\mathbf{a}_k(g) = -1$  for  $k = \pm 1$ ,  $\mathbf{a}_k(g) = 2$  for  $k = 0$ , and  $\mathbf{a}_k(g) = 0$  in any other case. We remind that the quoted symbol is related to the classical discrete Laplacian in one dimension. Hence  $\|g\|_\alpha < \infty$  for any  $\alpha > 0$  and the remaining simple-loop conditions are easily verified (see Fig. 2). Then  $g \in \text{SL}^\alpha$  for any  $\alpha > 0$ . In this case we obtain  $B_g(\sigma, s) = 1$  and  $H_g(s) = 0$ , and the eigenvalues of  $T_n(g)$  can be explicitly determined as  $\lambda_j(T_n(g)) = g(\sigma_{j,n})$  (a well-known fact for any tridiagonal Toeplitz matrix [48, Sc.2]).

**Example 4.1.** For the numerical implementation of Theorem 2.2, we consider the generating function  $f + hg$ . We need to calculate the singular integral in  $\psi$ , which for this example can be simplified to

$$\psi(s) = \frac{\sin(s)}{\pi} \int_0^{2\pi} \frac{1}{f(\sigma) - f(s)} d\sigma.$$

For the  $k$ th term approximation we obtain

$$\begin{aligned} \lambda_j^{\text{SL}(1)} &= f(\sigma_{j,n}), \\ \lambda_j^{\text{SL}(2)} &= f(\sigma_{j,n}) + \mathbf{r}_1(\sigma_{j,n})h, \\ \lambda_j^{\text{SL}(3)} &= f(\sigma_{j,n}) + \mathbf{r}_1(\sigma_{j,n})h + \mathbf{r}_2(\sigma_{j,n})h^2. \end{aligned}$$



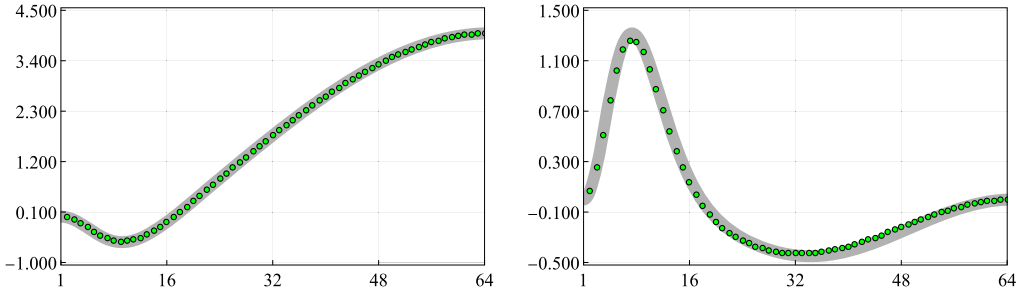


**Fig. 3.** [Example 4.1] Asymptotic expansion for the eigenvalues of  $T_n(f + hg)$ . The light thick gray curve is the term  $\tau_k$  in Theorem 2.2, and the green dots are the normalized errors  $NE_{j,n}^{SL(k)}$  for  $j = 1, \dots, n$ , and  $n = 64$ . The left graphic corresponds to the first term  $k = 1$  and the right one to the second  $k = 2$ .

**Table 1**

[Example 4.1] The maximum absolute errors  $AE_n^{SL(k)}$  and maximum normalized errors  $NE_n^{SL(k)}$  for  $k = 1, 2, 3$ , and different values of  $n$ , corresponding to the asymptotic expansion for the eigenvalues of  $T_n(f + hg)$  in Theorem 2.2.

$n$	$AE_n^{SL(1)}$	$NE_n^{SL(1)}$	$AE_n^{SL(2)}$	$NE_n^{SL(2)}$	$AE_n^{SL(3)}$	$NE_n^{SL(3)}$
32	$1.2092 \times 10^{-1}$	$3.9905 \times 10^0$	$1.1114 \times 10^{-3}$	$1.2103 \times 10^0$	$8.9892 \times 10^{-5}$	$3.2305 \times 10^0$
64	$6.1501 \times 10^{-2}$	$3.9976 \times 10^0$	$2.9830 \times 10^{-4}$	$1.2603 \times 10^0$	$1.2316 \times 10^{-5}$	$3.3823 \times 10^0$
128	$3.1003 \times 10^{-2}$	$3.9994 \times 10^0$	$7.7394 \times 10^{-5}$	$1.2879 \times 10^0$	$1.6228 \times 10^{-6}$	$3.4836 \times 10^0$
256	$1.5564 \times 10^{-2}$	$4.0000 \times 10^0$	$1.9728 \times 10^{-5}$	$1.3030 \times 10^0$	$2.0796 \times 10^{-7}$	$3.5301 \times 10^0$
512	$7.7972 \times 10^{-3}$	$4.0000 \times 10^0$	$4.9765 \times 10^{-6}$	$1.3096 \times 10^0$	$2.6386 \times 10^{-8}$	$3.5623 \times 10^0$
1024	$3.9024 \times 10^{-3}$	$4.0000 \times 10^0$	$1.2498 \times 10^{-6}$	$1.3130 \times 10^0$	$3.3384 \times 10^{-9}$	$3.5950 \times 10^0$
2048	$1.9522 \times 10^{-3}$	$4.0000 \times 10^0$	$3.1315 \times 10^{-7}$	$1.3147 \times 10^0$	$4.2375 \times 10^{-10}$	$3.6453 \times 10^0$
4096	$9.7632 \times 10^{-4}$	$4.0000 \times 10^0$	$7.8377 \times 10^{-8}$	$1.3156 \times 10^0$	$5.6220 \times 10^{-11}$	$3.8662 \times 10^0$
8192	$4.8822 \times 10^{-4}$	$4.0000 \times 10^0$	$1.9605 \times 10^{-8}$	$1.3160 \times 10^0$	$8.3189 \times 10^{-12}$	$4.5750 \times 10^0$

According to the results in Theorem 2.2, we must have  $E_{j,n}^{SL(k)} = O(h^k)$  uniformly in  $j$  for  $k = 1, 2, 3$ , more specifically the normalized errors

$$NE_{j,n}^{SL(k)} \equiv (n + 1)^k E_{j,n}^{SL(k)},$$

for  $k = 1, 2$ , are expected to be “close” to  $\tau_1$  and  $\tau_2$ , respectively. Let  $NE_n^{SL(k)} = \max\{NE_{j,n}^{SL(k)} : j = 1, \dots, n\}$ . Fig. 3 and Table 1 show the data.

**Example 4.2.** For the numerical implementation of Theorem 2.3, we consider the generating function  $f + h^h g$ . We need to calculate the singular integral in  $\varphi$ , which for this example can be simplified to

$$\varphi(s) = \frac{\sin(s)}{\pi} \int_0^{2\pi} \frac{1}{f(\sigma) - f(s) + 2 \cos(s) - 2 \cos(\sigma)} d\sigma.$$

Taking into account that the logarithm is relatively small for the matrix sizes considered, this time we arrange the  $k$ th term approximation in a different way

$$\lambda_j^{SL(1)} = f(\sigma_{j,n}) + g(\sigma_{j,n}),$$

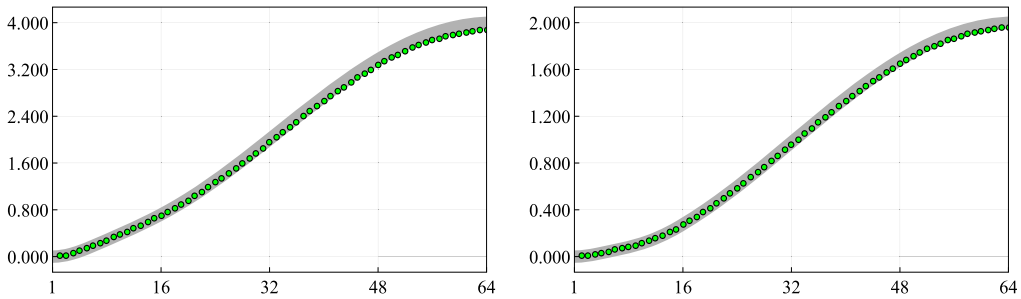


**Fig. 4.** [Example 4.2] Asymptotic expansion for the eigenvalues of the Toeplitz matrix  $T_n(f + h^k g)$ . The light thick gray curve is the term  $\mathfrak{s}_{1,1} + \mathfrak{s}_{1,0} \frac{1}{\log(h)}$  (left) and  $\mathfrak{s}_{2,2} + \mathfrak{s}_{2,1} \frac{1}{\log(h)} + \mathfrak{s}_{2,0} \frac{1}{\log^2(h)}$  (right) in Theorem 2.3, and the green dots are the normalized errors  $NE_{j,n}^{SL(k)}$  for  $j = 1, \dots, n$ , and  $n = 64$ . The left graphic corresponds to the first term  $k = 1$  and the right one to the second  $k = 2$ .

**Table 2**

[Example 4.2] The maximum absolute errors  $AE_n^{SL(k)}$  and maximum normalized errors  $NE_n^{SL(k)}$  for different values of  $n$ , and  $k = 1, 2, 3$ , corresponding to the asymptotic expansion for the eigenvalues of  $T_n(f + h^k g)$  in Theorem 2.3.

$n$	$AE_n^{SL(1)}$	$NE_n^{SL(1)}$	$AE_n^{SL(2)}$	$NE_n^{SL(2)}$	$AE_n^{SL(3)}$	$NE_n^{SL(3)}$
32	$4.0125 \times 10^{-1}$	$3.7870 \times 10^0$	$2.1631 \times 10^{-2}$	$1.9268 \times 10^0$	$7.7105 \times 10^{-4}$	$6.4822 \times 10^{-1}$
64	$2.4867 \times 10^{-1}$	$3.8720 \times 10^0$	$8.0703 \times 10^{-3}$	$1.9567 \times 10^0$	$1.7371 \times 10^{-4}$	$6.5583 \times 10^{-1}$
128	$1.4787 \times 10^{-1}$	$3.9250 \times 10^0$	$2.8028 \times 10^{-3}$	$1.9748 \times 10^0$	$3.5309 \times 10^{-5}$	$6.6038 \times 10^{-1}$
256	$8.5438 \times 10^{-2}$	$3.9570 \times 10^0$	$9.2570 \times 10^{-4}$	$1.9856 \times 10^0$	$6.6746 \times 10^{-6}$	$6.6307 \times 10^{-1}$
512	$4.8362 \times 10^{-2}$	$3.9757 \times 10^0$	$2.9474 \times 10^{-4}$	$1.9919 \times 10^0$	$1.1963 \times 10^{-6}$	$6.6465 \times 10^{-1}$
1024	$2.6962 \times 10^{-2}$	$3.9865 \times 10^0$	$9.1280 \times 10^{-5}$	$1.9955 \times 10^0$	$2.0621 \times 10^{-7}$	$6.6654 \times 10^{-1}$
2048	$1.4858 \times 10^{-2}$	$3.9926 \times 10^0$	$2.7663 \times 10^{-5}$	$1.9975 \times 10^0$	$3.4466 \times 10^{-8}$	$6.6877 \times 10^{-1}$
4096	$8.1128 \times 10^{-3}$	$3.9959 \times 10^0$	$8.2384 \times 10^{-6}$	$1.9986 \times 10^0$	$5.6243 \times 10^{-9}$	$6.7206 \times 10^{-1}$
8192	$4.3970 \times 10^{-3}$	$3.9978 \times 10^0$	$2.4184 \times 10^{-6}$	$1.9993 \times 10^0$	$9.0135 \times 10^{-10}$	$6.7748 \times 10^{-1}$

$$\lambda_j^{SL(2)} = f(\sigma_{j,n}) + g(\sigma_{j,n}) + \mathfrak{s}_{1,1}(\sigma_{j,n})h \log(h) + \mathfrak{s}_{1,0}(\sigma_{j,n})h,$$

$$\lambda_j^{SL(3)} = f(\sigma_{j,n}) + g(\sigma_{j,n}) + \mathfrak{s}_{1,1}(\sigma_{j,n})h \log(h) + \mathfrak{s}_{1,0}(\sigma_{j,n})h + \mathfrak{s}_{2,2}(\sigma_{j,n})h^2 \log^2(h) + \mathfrak{s}_{2,1}(\sigma_{j,n})h^2 \log(h) + \mathfrak{s}_{2,0}(\sigma_{j,n})h^2.$$

According to the results in Theorem 2.2, we have the bound  $E_{j,n}^{SL(k)} = O(h^k |\log^k(h)|)$  uniformly in  $j = 1, \dots, n$ , for  $k = 1, 2, 3$ ; more specifically this time the normalized errors are given by

$$NE_{j,n}^{SL(k)} = \frac{(n+1)^k}{\log^k(n+1)} E_{j,n}^{SL(k)} \quad (k = 1, 2),$$

and are expected to be “close” to the functions  $\mathfrak{s}_{1,1} + \mathfrak{s}_{1,0} \frac{1}{\log(h)}$  and  $\mathfrak{s}_{2,2} + \mathfrak{s}_{2,1} \frac{1}{\log(h)} + \mathfrak{s}_{2,0} \frac{1}{\log^2(h)}$ , respectively. Fig. 4 and Table 2 show the data.

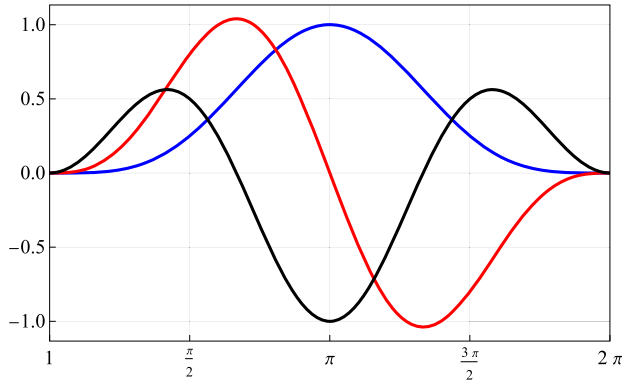


Fig. 5. [Example 4.3] The momentary symbol  $F_n(\sigma) = f_2(\sigma) + \alpha_1 f_1(\sigma)h^2 + \alpha_0 f_0(\sigma)h^4$  with  $f_k(\sigma) \equiv (2 - 2 \cos(\sigma))^k$ , and its first two derivatives for  $\alpha_1 = 3, \alpha_2 = 2$ , and  $n = 32$ . The blue, red, and black curves are  $F_n/\|F_n\|_\infty, F'_n/\|F'_n\|_\infty$ , and  $F''_n/\|F''_n\|_\infty$ , respectively.

4.2. A substantial improvement of the algorithm in [3]

**Example 4.3.** For  $k \in \mathbb{Z}_+$  let  $f_k(\sigma) \equiv (2 - 2 \cos(\sigma))^k$  and  $\alpha_k \in \mathbb{R}$ . Consider the (momentary) symbol

$$F_n(\sigma) \equiv f_2(\sigma) + \alpha_1 f_1(\sigma)h^2 + \alpha_0 f_0(\sigma)h^4, \tag{4.3}$$

see Fig. 5. The related Toeplitz matrices  $T_n(F_n)$  appear when discretizing differential equations with the Finite Differences method.

The functions  $f_k$  with  $k \neq 2$ , do not belong to  $SL^\alpha$  for any  $\alpha$ , thus  $F_n$  do not fully satisfy our hypothesis and we cannot apply our theoretical results. Nevertheless, according to [28,30] we can expect an expansion of the form

$$\lambda_j(T_n(F_n)) = f_2(\sigma_{j,n}) + \sum_{\ell=1}^3 c_\ell(\sigma_{j,n})h^\ell + O(h^4). \tag{4.4}$$

Moreover, the first few eigenvalues have order  $O(h^4)$  (coinciding with the classical results of Parter [52]).

As a consequence, for those eigenvalues (4.4) will produce an approximation with an error comparable to the eigenvalue itself. To appreciate this phenomenon, we consider the respective relative errors

$$RE_{j,n}^{SL(k)} \equiv \frac{|\lambda_j(T_n(F_n)) - \lambda_j^{SL(k)}(T_n(F_n))|}{|\lambda_j(T_n(F_n))|} = \frac{AE_{j,n}^{SL(k)}}{|\lambda_j(T_n(F_n))|}.$$

Hence, according to [28,30] we expect that the expansion (4.4) produces acceptable relative errors only for  $j > \log(n)$ .

We now proceed to determine the continuous functions  $c_\ell$  following the algorithm proposed in [3,4,20]. This algorithm is a clever interplay between extrapolation and interpolation.

For given natural numbers  $m$  and  $n_0$ , the extrapolation step, gives us a numerical approximation of  $c_\ell$  ( $\ell = 1, \dots, m - 1$ ) at the regular mesh  $\pi j h_0$  ( $j = 1, \dots, n_0$ ) of the interval  $[0, \pi]$ , where  $h_0 \equiv 1/(n_0 + 1)$ . Then, in the interpolation step, we use certain polynomial interpolation to obtain the value of  $c_\ell$  at any point in the interval  $[0, \pi]$ .

We noticed that this algorithm can produce large errors when evaluating  $c_\ell$  close to the extreme points  $\{0, \pi\}$ , i.e.  $10^3$  bigger than the rest. As we can see in Theorems 2.2 and 2.3, the functions  $c_\ell$  are a sum of products of  $H_f$ , the symbol, and its derivatives, and we must have  $H_f(0) = H_f(\pi) = 0$  (see (2.2)). Therefore, taking into account the nature of the symbol (4.3) we have

$$\begin{aligned} c_2(0) = \alpha_1 f_1(0) = 0, & \quad c_2(\pi) = \alpha_1 f_1(\pi) = 4\alpha_1, \\ c_4(0) = \alpha_0 f_0(0) = 0, & \quad c_4(\pi) = \alpha_0 f_0(\pi) = \alpha_0, \end{aligned}$$

while  $c_\ell(0) = c_\ell(\pi) = 0$  for  $\ell \neq 2, 4$ . Hence we propose here to include those values in the interpolation step and to look for an optimal number of interpolated points. Our numerical results reveal that the errors in the extreme points almost disappear and that the approximation of the functions  $c_\ell$  improves in such a way that the respective errors behave better when  $\ell$  increases (see Figs. 6, 7, and Tables 3, 4). We emphasize that this contribution represents a substantial improvement to the algorithm presented in [3] and it is a general idea to be used in various contexts.

More specifically, let  $\lambda_j^{NA(k)}(T_n(F_n))$  be the  $k$ th-term numerical approximation of the eigenvalue  $\lambda_j(T_n(F_n))$ , given by (4.4), that is

$$\lambda_j^{NA(k)}(T_n(F_n)) \equiv f_2(\sigma_{j,n}) + \sum_{\ell=1}^{k-1} c_\ell^{NA}(\sigma_{j,n}) h^\ell,$$

where the functions  $c_\ell^{NA}$  are obtained with the numerical algorithm. Let

$$E_{j,n}^{NA(k)} \equiv \lambda_j(T_n(F_n)) - \lambda_j^{NA(k)}(T_n(F_n)), \quad AE_n^{NA(k)} \equiv \max\{|E_{j,n}^{NA(k)}| : j = 1, \dots, n\},$$

be the corresponding errors. According to [3, Th.3] we will have the bound  $AE_n^{NA(k)} = O(h_0^k h)$ , thus let

$$NE_n^{NA(k)} \equiv (n_0 + 1)^k (n + 1) AE_n^{NA(k)}$$

be the respective normalized error. Figs. 6, 7, and Tables 3, 4, show the data.

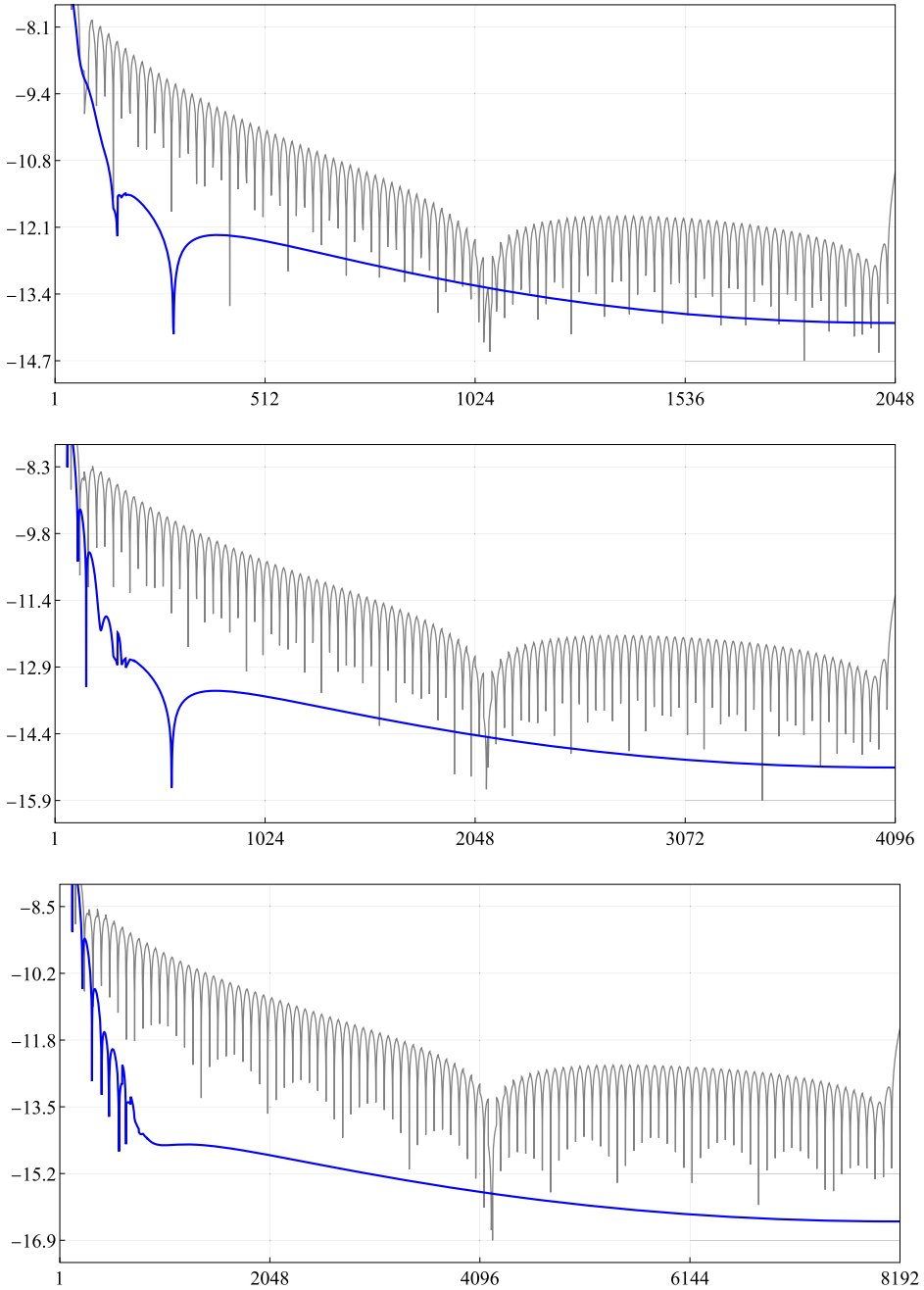


**Fig. 6.** [Example 4.3] The log-scaled eigenvalue relative errors  $\log_{10}(\text{RE}_{j,n}^{\text{NA}(k)})$  for  $k = 4$ ,  $n = 2048$  (top),  $n = 4096$  (middle), and  $n = 8192$  (bottom). We worked with a regular mesh of size  $n_0 = 100$  and the momentary symbol  $F_n(\sigma) = (2 - 2 \cos(\sigma))^2 + 3(2 - 2 \cos(\sigma))h^2 + 2h^4$ , see (4.3). The gray and blue curves correspond to the errors produced with the algorithm in [3,4,20] and to our modification, respectively.

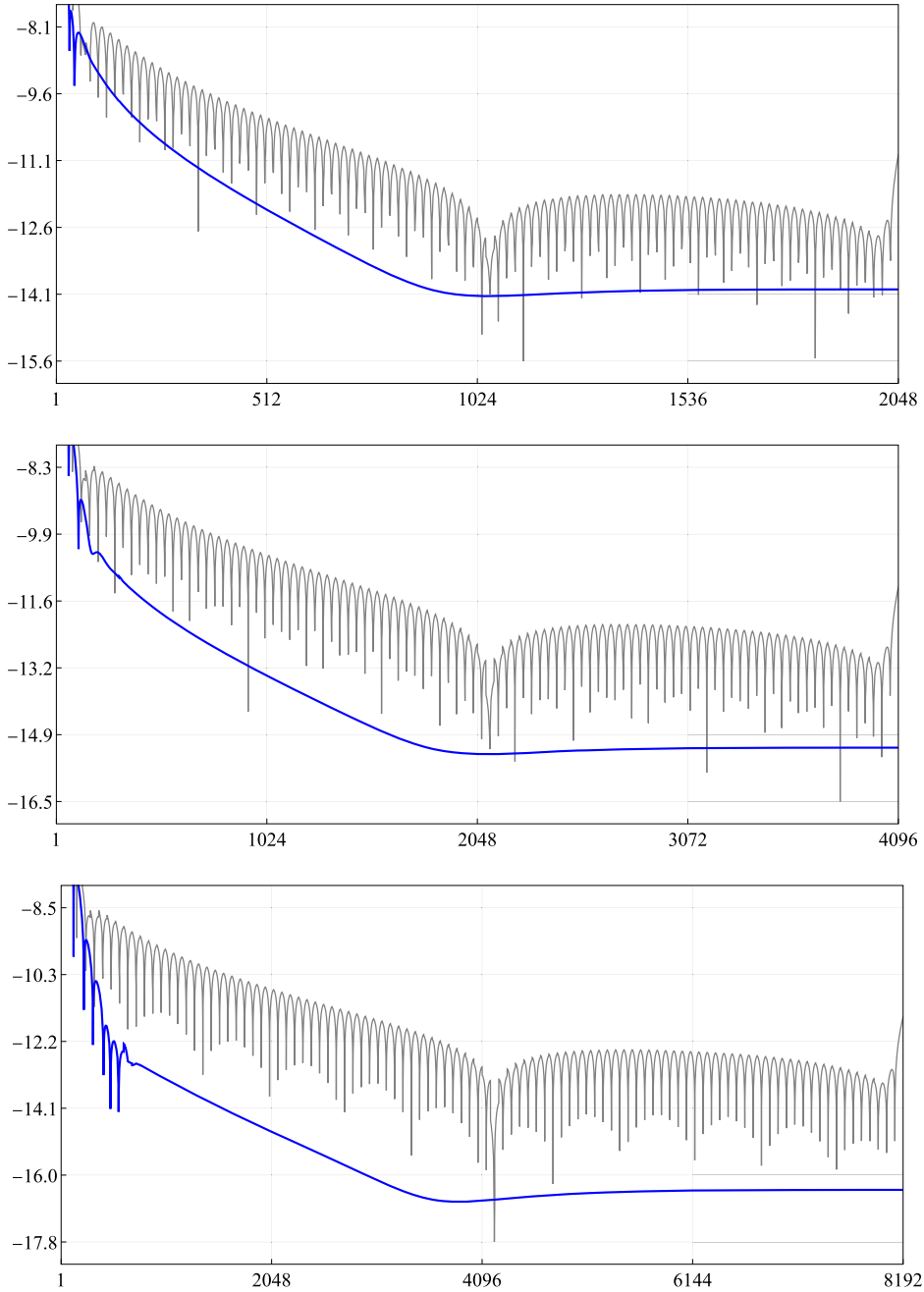


**Fig. 7.** [Example 4.3] The log-scaled eigenvalue relative errors  $\log_{10}(\text{RE}_{j,n}^{\text{NA}(k)})$  for  $k = 4$ ,  $n = 2048$  (top),  $n = 4096$  (middle), and  $n = 8192$  (bottom). We worked with a regular mesh of size  $n_0 = 100$  and the momentary symbol  $F_n(\sigma) = (2 - 2 \cos(\sigma))^2 - 3(2 - 2 \cos(\sigma))h^2 + 5h^4$ , see (4.3). The gray and blue curves correspond to the errors produced with the algorithm in [3,4,20] and to our modification, respectively.

**Table 3**

[Example 4.3] The maximum eigenvalue errors  $AE_n^{NA(k)}$  and normalized errors  $NE_n^{NA(k)}$  for an expansion of  $k = 1, \dots, 4$ , terms, corresponding to the momentary symbol  $F_n(\sigma) = (2 - 2 \cos(\sigma))^2 + 3(2 - 2 \cos(\sigma))h^2 + 2h^4$ , see (4.3), with different values of  $n$  and a regular mesh of  $n_0 = 100$  points.

$n$	256	512	1024	2048	4096	8192
$AE_n^{NA(1)}$	$5.4089 \times 10^{-3}$	$2.8591 \times 10^{-3}$	$1.4689 \times 10^{-3}$	$7.4434 \times 10^{-4}$	$3.7466 \times 10^{-4}$	$1.8795 \times 10^{-4}$
$NE_n^{NA(1)}$	$1.4040 \times 10^2$	$1.4814 \times 10^2$	$1.5206 \times 10^2$	$1.5404 \times 10^2$	$1.5503 \times 10^2$	$1.5553 \times 10^2$
$AE_n^{NA(2)}$	$3.8731 \times 10^{-5}$	$9.8762 \times 10^{-6}$	$2.4925 \times 10^{-6}$	$6.2602 \times 10^{-7}$	$1.5686 \times 10^{-7}$	$3.9260 \times 10^{-8}$
$NE_n^{NA(2)}$	$1.0154 \times 10^2$	$5.1683 \times 10^1$	$2.6062 \times 10^1$	$1.3085 \times 10^1$	$6.5558 \times 10^0$	$3.2812 \times 10^0$
$AE_n^{NA(3)}$	$9.3695 \times 10^{-8}$	$1.1764 \times 10^{-8}$	$1.4767 \times 10^{-9}$	$1.8484 \times 10^{-10}$	$2.3122 \times 10^{-11}$	$2.8913 \times 10^{-12}$
$NE_n^{NA(3)}$	$2.4809 \times 10^1$	$6.2178 \times 10^0$	$1.5595 \times 10^0$	$3.9021 \times 10^{-1}$	$9.7602 \times 10^{-2}$	$2.4406 \times 10^{-2}$
$AE_n^{NA(4)}$	$4.4299 \times 10^{-9}$	$3.0154 \times 10^{-10}$	$2.0443 \times 10^{-11}$	$1.2969 \times 10^{-12}$	$1.7757 \times 10^{-13}$	$1.6021 \times 10^{-13}$
$NE_n^{NA(4)}$	$1.1847 \times 10^2$	$1.6097 \times 10^1$	$2.1805 \times 10^0$	$2.7653 \times 10^{-1}$	$7.5705 \times 10^{-2}$	$1.3659 \times 10^{-1}$

**Table 4**

[Example 4.3] The maximum eigenvalue errors  $AE_n^{NA(k)}$  and normalized errors  $NE_n^{NA(k)}$  for an expansion of  $k = 1, \dots, 4$ , terms, corresponding to the momentary symbol  $F_n(\sigma) = (2 - 2 \cos(\sigma))^2 - 3(2 - 2 \cos(\sigma))h^2 + 5h^4$  (see (4.3)) with different values of  $n$  and a regular mesh of  $n_0 = 100$  points.

$n$	256	512	1024	2048	4096	8192
$AE_n^{NA(1)}$	$5.4089 \times 10^{-3}$	$2.8591 \times 10^{-3}$	$1.4689 \times 10^{-3}$	$7.4434 \times 10^{-4}$	$3.7466 \times 10^{-4}$	$1.8795 \times 10^{-4}$
$NE_n^{NA(1)}$	$1.4040 \times 10^2$	$1.4814 \times 10^2$	$1.5206 \times 10^2$	$1.5404 \times 10^2$	$1.5503 \times 10^2$	$1.5553 \times 10^2$
$AE_n^{NA(2)}$	$3.8731 \times 10^{-5}$	$9.8762 \times 10^{-6}$	$2.4925 \times 10^{-6}$	$6.2602 \times 10^{-7}$	$1.5686 \times 10^{-7}$	$3.9260 \times 10^{-8}$
$NE_n^{NA(2)}$	$1.0154 \times 10^2$	$5.1683 \times 10^1$	$2.6062 \times 10^1$	$1.3085 \times 10^1$	$6.5558 \times 10^0$	$3.2812 \times 10^0$
$AE_n^{NA(3)}$	$9.3695 \times 10^{-8}$	$1.1764 \times 10^{-8}$	$1.4767 \times 10^{-9}$	$1.8484 \times 10^{-10}$	$2.3122 \times 10^{-11}$	$2.8913 \times 10^{-12}$
$NE_n^{NA(3)}$	$2.4809 \times 10^1$	$6.2178 \times 10^0$	$1.5595 \times 10^0$	$3.9021 \times 10^{-1}$	$9.7602 \times 10^{-2}$	$2.4406 \times 10^{-2}$
$AE_n^{NA(4)}$	$4.4299 \times 10^{-9}$	$3.0154 \times 10^{-10}$	$2.0443 \times 10^{-11}$	$1.2969 \times 10^{-12}$	$1.7757 \times 10^{-13}$	$1.6021 \times 10^{-13}$
$NE_n^{NA(4)}$	$1.1847 \times 10^2$	$1.6097 \times 10^1$	$2.1805 \times 10^0$	$2.7653 \times 10^{-1}$	$7.5705 \times 10^{-2}$	$1.3659 \times 10^{-1}$

### 4.3. Multidimensional block setting: eigenvalue computation

In this subsection, we provide some useful background knowledge regarding multilevel block Toeplitz matrices.

We let  $L^1([-\pi, \pi]^k, \mathbb{C}^{m \times m})$  be the Banach space of all  $m$ -by- $m$  matrix valued Lebesgue integrable functions over  $[-\pi, \pi]^k$ , equipped with the following norm

$$\|f\|_{L^1} = \frac{1}{(2\pi)^k} \int_{[-\pi, \pi]^k} \|f(\boldsymbol{\theta})\|_{\text{tr}} \, d\boldsymbol{\theta} < \infty,$$

where  $\|A\|_{\text{tr}} \equiv \sum_{j=1}^m \sigma_j(A)$  denotes the trace norm of  $A \in \mathbb{C}^{m \times m}$ ,  $\sigma_j(A)$ ,  $j = 1, \dots, m$ , being the singular values of  $A$ .

The multi-index  $\mathbf{n} = (n_1, n_2, \dots, n_k)$  is defined with each  $n_j$  being a positive integer. When writing the expression  $\mathbf{n} \rightarrow \infty$  we mean that every component of the vector  $\mathbf{n}$  tends to infinity, i.e.,  $\min_{1 \leq j \leq k} n_j \rightarrow \infty$ . Furthermore, in the current multilevel context, it is convenient to use the Kronecker tensor product  $\otimes$  for matrices, where  $A \otimes B$  denotes the block matrix of the form  $(a_{i,j}B)$  with  $A = (a_{i,j})$ . In a function setting, writing  $f = f_1 \otimes f_2$  indicates a basic separable function  $f(x, y) = f_1(x)f_2(y)$  where  $x$  lies in the domain of  $f_1$  and  $y$  lies in the domain of  $f_2$ .

Let  $f: [-\pi, \pi]^k \rightarrow \mathbb{C}^{m \times m}$  be a function belonging to  $L^1([-\pi, \pi]^k, \mathbb{C}^{m \times m})$ , and periodically extended to  $\mathbb{R}^k$ . We define  $T_{(\mathbf{n}, m)}[f]$  the multilevel block Toeplitz matrix of dimensions  $mN(\mathbf{n}) \times mN(\mathbf{n})$ , with  $N(\mathbf{n}) = n_1 n_2 \cdots n_k$  as follows

$$T_{(\mathbf{n}, m)}[f] = \sum_{|r_1| < n_1} \cdots \sum_{|r_k| < n_k} J_{n_1}^{r_1} \otimes \cdots \otimes J_{n_k}^{r_k} \otimes A_{(\mathbf{r})}, \quad \mathbf{r} = (r_1, r_2, \dots, r_k) \in \mathbb{Z}^k,$$

where

$$A_{(\mathbf{r})} = \frac{1}{(2\pi)^k} \int_{[-\pi, \pi]^k} f(\boldsymbol{\theta}) e^{i\langle \mathbf{r}, \boldsymbol{\theta} \rangle} d\boldsymbol{\theta},$$

with  $\langle \mathbf{r}, \boldsymbol{\theta} \rangle = \sum_{t=1}^k r_t \theta_t$ , is the Fourier coefficient matrix of  $f$  and  $J_n^r$  is the  $n \times n$  matrix whose  $(\ell, s)$ -th entry equals 1 if  $\ell - s = r$  and 0 otherwise, that is,  $J_n^r$  is the  $n \times n$  Toeplitz matrix with entries 1 in the  $r$ th diagonal and zero elsewhere.

We indicate by  $\{T_{(\mathbf{n}, m)}[f]\}_{\mathbf{n}}$  the matrix-sequence whose elements are the matrices  $T_{(\mathbf{n}, m)}[f]$ . The function  $f$  is called the *generating function* of  $T_{(\mathbf{n}, m)}[f]$ .

If  $f$  is Hermitian-valued almost everywhere (a.e.), then  $T_{(\mathbf{n}, m)}[f]$  is Hermitian for any choice of  $\mathbf{n}$  and  $m$ . If  $f$  is Hermitian-valued and nonnegative a.e., but not identically zero a.e., then  $T_{(\mathbf{n}, m)}[f]$  is Hermitian positive definite  $\forall \mathbf{n}, m$ . If  $f$  is Hermitian-valued and even a.e., then  $T_{(\mathbf{n}, m)}[f]$  is real and symmetric for any choice of  $\mathbf{n}$  and  $m$  [45,53,54].

**Example 4.4.** With respect to the previous notation, we have

$$T_{(\mathbf{n}, m)}[f_1 \otimes f_2] = T_{(\mathbf{n}[1], m)}[f_1] \otimes T_{(\mathbf{n}[2], m)}[f_2],$$

with  $\mathbf{n} = (\mathbf{n}[1], \mathbf{n}[2])$ ,  $f_1$  being  $k_1$  variate and  $f_2$  being  $k_2$  variate, with  $\mathbf{n}[r]$  being a multi-index of cardinality  $k_r$ ,  $r = 1, 2$ .

For the eigenvalue expansions in a multilevel setting, in this example we consider  $T_{(\mathbf{n}, 1)}[f_h]$  with  $\mathbf{n} = (n_1, n_2)$ ,  $n_1 = n_2 = n$ ,  $\gamma = 1, 3/2, 2$ ,

$$f_h(\boldsymbol{\theta}) \equiv \sum_{r=1}^2 [f_{0,r}(\theta_r) + h^\gamma f_{1,r}(\theta_r)], \tag{4.5}$$

$$f_{0,r}(\theta_r) = (2 - 2 \cos(\theta_r))^{\frac{\gamma}{2}}, \quad f_{1,r}(\theta_r) = 20 + r \cos(\theta_r) + (r + 1) \cos(2\theta_r),$$

$r = 1, 2$ . See Fig. 8. In such a setting, arising e.g. in the numerical approximation of operators of the form  $\sum_{r=1}^k \frac{\partial^\gamma}{\partial x_r^\gamma}$ ,  $\gamma$  is an even positive integer or  $\gamma \in [1, 2)$  in the symmetric fractional case, owing to the tensor structure of the given matrices. Of course, with regard to equation (4.5), any parameter  $\gamma > 0$  is of interest in concrete applications because standard Finite Difference approximations of any higher order operator also of fractional type are included in formula (4.5).



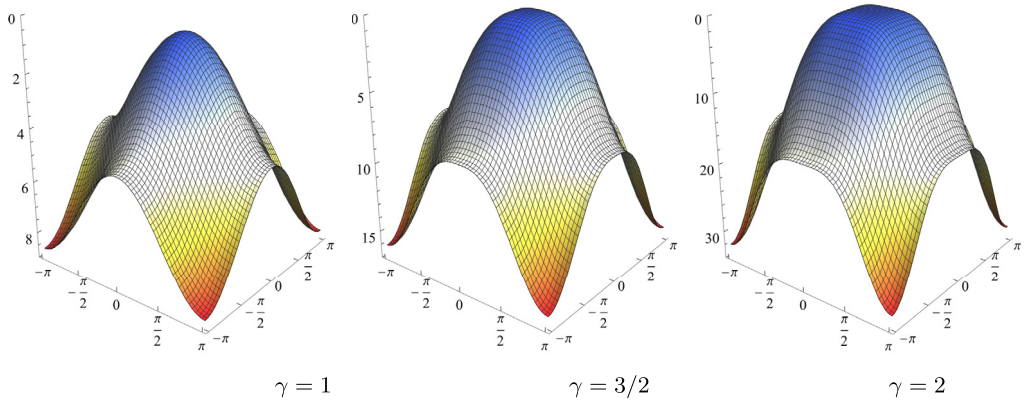


Fig. 8. [Example 4.4] The generating function  $f_h(\theta_1, \theta_2)$  in (4.5) plotted on  $[-\pi, \pi]^2$ , for  $n = 64$  and different values of  $\gamma$ .

The eigenvalues of  $T_{(n,1)}[f_h]$  take the form

$$\lambda_{j_1}(T_n(q_1)) + \lambda_{j_2}(T_n(q_2)), \quad 1 \leq j_1, j_2 \leq n, \tag{4.6}$$

where  $\lambda_j(T_n(q_r))$  is the  $j$ th eigenvalue of the unilevel Toeplitz matrix  $T_n(q_r)$  with  $q_r(\theta_r) \equiv f_{0,r}(\theta_r) + h^\gamma f_{1,r}(\theta_r)$ ,  $r = 1, 2$ , for which the asymptotical expansion has been worked out previously.

For  $m = 1$  and  $\mathbf{n} = (n, n)$ , the resulting multilevel block Toeplitz matrix is

$$T_{(n,1)}[f_h] = \sum_{r_1=-n+1}^{n-1} \sum_{r_2=-n+1}^{n-1} J_n^{r_1} \otimes J_n^{r_2} \otimes A_{(r_1,r_2)},$$

where the Fourier coefficient matrix  $A_{(r_1,r_2)}$  turns out to be

$$A_{(r_1,r_2)} = \delta_{r_2,0} \mathbf{a}_{r_1}(f_{0,1}) + \delta_{r_2,0} \mathbf{a}_{r_1}(f_{1,1})h^\gamma + \delta_{r_1,0} \mathbf{a}_{r_2}(f_{0,2}) + \delta_{r_1,0} \mathbf{a}_{r_2}(f_{1,2})h^\gamma,$$

and  $\delta_{\cdot,\cdot}$  is the usual delta Kronecker function.

The functions  $q_1, q_2$  do not belong to  $SL^\alpha$  for any  $\alpha$ , thus we cannot apply our theoretical results, but as in the previous example, there is numerical evidence suggesting that, nevertheless we can expect an eigenvalue expansion of the form

$$\lambda_j(T_n(q_r)) = f_{0,r}(\sigma_{j,n}) + \sum_{\ell=1}^{m-1} \mathbf{u}_\ell(\sigma_{j,n})h^{\ell\beta} + O(h^{m\beta}), \tag{4.7}$$

for  $r = 1, 2$ ,  $\sigma_{j,n} = \pi jh$ , and some constants  $\beta \in (0, 1]$  and  $m \in \mathbb{N}$ .

According to (4.6) the eigenvalues of  $T_{(\mathbf{n},1)}[f_h]$  can be arranged in the  $n \times n$  matrix  $\lambda(T_{(\mathbf{n},1)}[f_h])$  given by

$$\begin{bmatrix} \lambda_1(T_n(q_1)) + \lambda_1(T_n(q_2)) & \lambda_1(T_n(q_1)) + \lambda_2(T_n(q_2)) & \cdots & \lambda_1(T_n(q_1)) + \lambda_n(T_n(q_2)) \\ \lambda_2(T_n(q_1)) + \lambda_1(T_n(q_2)) & \lambda_2(T_n(q_1)) + \lambda_2(T_n(q_2)) & \cdots & \lambda_2(T_n(q_1)) + \lambda_n(T_n(q_2)) \\ \vdots & \vdots & \ddots & \vdots \\ \lambda_n(T_n(q_1)) + \lambda_n(T_n(q_2)) & \lambda_1(T_n(q_1)) + \lambda_2(T_n(q_2)) & \cdots & \lambda_n(T_n(q_1)) + \lambda_n(T_n(q_2)) \end{bmatrix}. \tag{4.8}$$

For the numerical experiments let  $\lambda_j^{\text{NA}(k)}(T_n(q_r))$  be the  $k$ th-term numerical approximation of the eigenvalue  $\lambda_j(T_n(q_r))$ , given by (4.7), that is

$$\lambda_j^{\text{NA}(k)}(T_n(q_r)) = f_{0,r}(\sigma_{j,n}) + \sum_{\ell=1}^{k-1} u_\ell^{\text{NA}}(\sigma_{j,n}) h^{\ell\beta},$$

where the functions  $u_\ell^{\text{NA}}$  are obtained with the numerical algorithm. The parameter  $\beta$  must be determined for each example. Similarly, let

$$\lambda_{\mathbf{j}}^{\text{NA}(k)}(T_{(\mathbf{n},1)}[f_h]) = \lambda_{j_1}^{\text{NA}(k)}(T_n(q_1)) + \lambda_{j_2}^{\text{NA}(k)}(T_n(q_2)), \quad \mathbf{j} = (j_1, j_2),$$

be the respective  $k$ th-term approximation for the  $\mathbf{j}$ th eigenvalue of  $T_{(\mathbf{n},1)}[f_h]$ .

Note that the eigenvalues  $\lambda_{\mathbf{j}}^{\text{NA}(k)}(T_{(\mathbf{n},1)}[f_h])$  are real-valued and can be arranged in non-decreasing order. For the linearly ordered eigenvalues, Fig. 9 shows the absolute individual errors

$$\text{AE}_{(\mathbf{j},\mathbf{n})}^{\text{NA}(k)} \equiv |\lambda_{\mathbf{j}}(T_{(\mathbf{n},1)}[f_h]) - \lambda_{\mathbf{j}}^{\text{NA}(k)}(T_{(\mathbf{n},1)}[f_h])|,$$

for  $\mathbf{n} = (8192, 8192)$  and different values of  $\gamma$ . Since in this case, the Toeplitz multilevel matrix  $T_{(\mathbf{n},1)}[f_h]$  has  $N(8192) = 8192^2 = 67\,108\,864$  eigenvalues, its calculation is a real challenge. Fig. 10 shows the same as Fig. 9 but with the eigenvalues arranged in its matrix form  $\lambda(T_{(\mathbf{n},1)}[f_h])$  given by (4.8).

Tables 5, 6, and 7 show the maximum absolute and normalized eigenvalue errors

$$\begin{aligned} \text{AE}_{(\mathbf{n})}^{\text{NA}(k)} &\equiv \max\{\text{AE}_{(\mathbf{j},\mathbf{n})}^{\text{NA}(k)} : 1 \leq j_1, j_2 \leq n, \mathbf{j} = (j_1, j_2)\}, \\ \text{NE}_{(\mathbf{n})}^{\text{NA}(k)} &\equiv \text{AE}_{(\mathbf{n})}^{\text{NA}(k)} (n + 1)^{\beta k}, \end{aligned}$$

for different combinations of  $\gamma$ ,  $\beta$ , and  $k$ . According to (4.7), we expect for  $\text{NE}_{(\mathbf{n})}^{\text{NA}(k)}$  to be bounded with respect to  $\mathbf{n}$ , a fact that can be nicely seen in the mentioned tables.

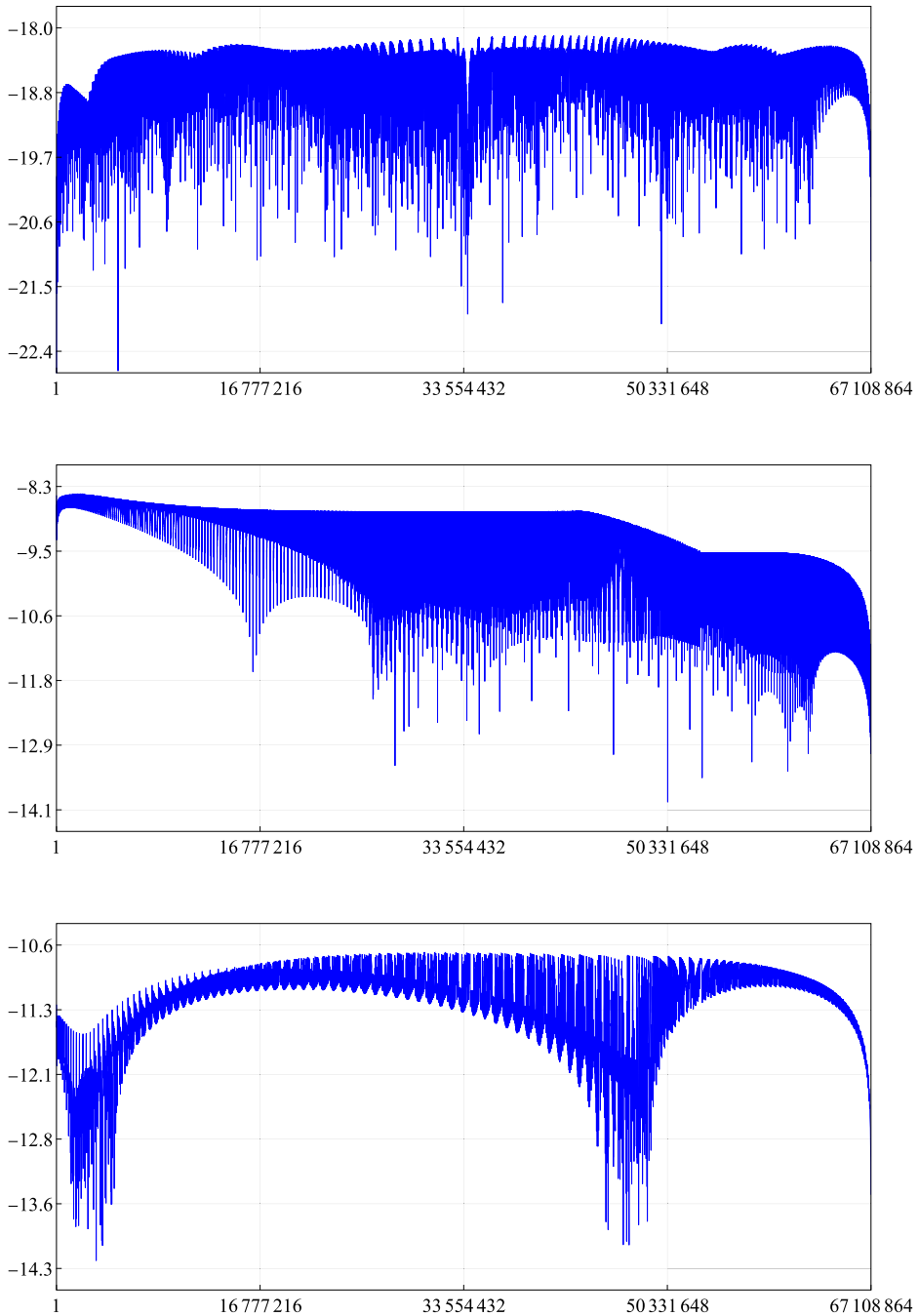


**Fig. 9.** [Example 4.4] For the multilevel Toeplitz matrix  $T_{(n,1)}[f_h]$  with generating function  $f_h(\theta_1, \theta_2)$  in (4.5) and its linearly ordered eigenvalues, the figure shows the 10-base logarithm of the absolute individual eigenvalue errors  $AE_{(j,n)}^{NA(k)}$  for  $\mathbf{n} = (8192, 8192)$  and different combinations of  $k, \beta$ , and  $\gamma$ . Top:  $\gamma = 1, \beta = 1, k = 5$ , middle:  $\gamma = 3/2, \beta = 1/2, k = 3$ , and bottom:  $\gamma = 2, \beta = 1, k = 3$ . The order of the matrix  $T_{(n,1)}[f_h]$  is  $N(\mathbf{n}) = 8192^2 = 67\,108\,864$ .

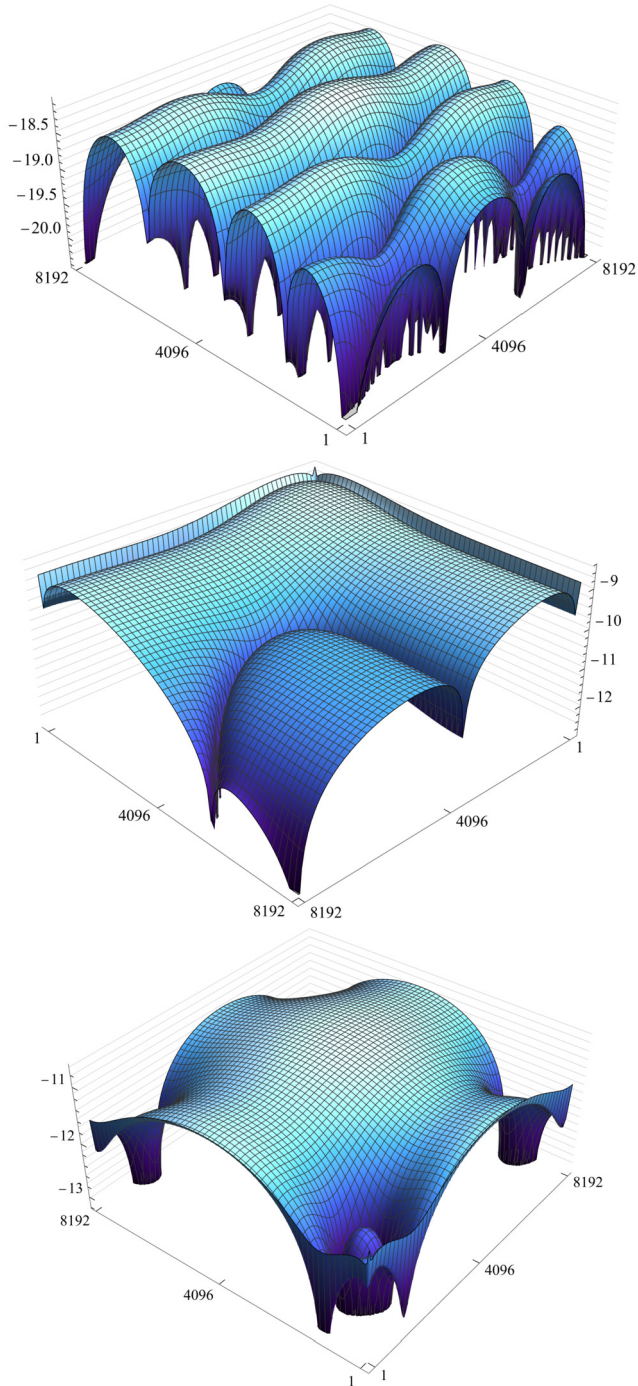


**Fig. 10.** [Example 4.4] For the multilevel Toeplitz matrix  $T_{(n,1)}[f_h]$  with generating function  $f_h(\theta_1, \theta_2)$  in (4.5) and its matrix arranged eigenvalues (see (4.8)), the figure shows the 10-base logarithm of the absolute individual eigenvalue errors  $AE_{(j,n)}^{NA(k)}$  for  $\mathbf{n} = (8192, 8192)$  and different combinations of  $k$ ,  $\beta$ , and  $\gamma$ . Top:  $\gamma = 1$ ,  $\beta = 1$ ,  $k = 5$ , middle:  $\gamma = 3/2$ ,  $\beta = 1/2$ ,  $k = 3$ , and bottom:  $\gamma = 2$ ,  $\beta = 1$ ,  $k = 3$ .

**Table 5**

[Example 4.4] For the multilevel Toeplitz matrix  $T_{(n,1)}[f_h]$  with generating function  $f_h(\theta_1, \theta_2)$  in (4.5), the maximum absolute and normalized eigenvalue errors  $AE_{(n)}^{NA(k)}$  and  $NE_{(n)}^{NA(k)}$ , respectively, for  $\gamma = 1, \beta = 1$ , and different values of  $k$ .

$n$	$256^2$	$512^2$	$1024^2$	$2048^2$	$4096^2$	$8192^2$
$AE_{(n)}^{NA(1)}$	$1.8676 \times 10^{-1}$	$9.3566 \times 10^{-2}$	$4.6829 \times 10^{-2}$	$2.3426 \times 10^{-2}$	$1.1716 \times 10^{-2}$	$5.8587 \times 10^{-3}$
$NE_{(n)}^{NA(1)}$	$4.7998 \times 10^1$	$4.8000 \times 10^1$	$4.8000 \times 10^1$	$4.8000 \times 10^1$	$4.8000 \times 10^1$	$4.8000 \times 10^1$
$AE_{(n)}^{NA(2)}$	$1.5140 \times 10^{-4}$	$3.7999 \times 10^{-5}$	$9.5182 \times 10^{-6}$	$2.3819 \times 10^{-6}$	$5.9576 \times 10^{-7}$	$1.4898 \times 10^{-7}$
$NE_{(n)}^{NA(2)}$	$1.0000 \times 10^1$	$1.0000 \times 10^1$	$1.0000 \times 10^1$	$1.0000 \times 10^1$	$1.0000 \times 10^1$	$1.0000 \times 10^1$
$AE_{(n)}^{NA(3)}$	$2.7221 \times 10^{-7}$	$3.4139 \times 10^{-8}$	$4.2740 \times 10^{-9}$	$5.3466 \times 10^{-10}$	$6.6858 \times 10^{-11}$	$8.3589 \times 10^{-12}$
$NE_{(n)}^{NA(3)}$	$4.6207 \times 10^0$	$4.6089 \times 10^0$	$4.6027 \times 10^0$	$4.5995 \times 10^0$	$4.5978 \times 10^0$	$4.5970 \times 10^0$
$AE_{(n)}^{NA(4)}$	$3.5980 \times 10^{-9}$	$2.2690 \times 10^{-10}$	$1.4245 \times 10^{-11}$	$8.9231 \times 10^{-13}$	$5.5832 \times 10^{-14}$	$3.4913 \times 10^{-15}$
$NE_{(n)}^{NA(4)}$	$1.5696 \times 10^1$	$1.5715 \times 10^1$	$1.5724 \times 10^1$	$1.5728 \times 10^1$	$1.5731 \times 10^1$	$1.5731 \times 10^1$
$AE_{(n)}^{NA(5)}$	$2.0263 \times 10^{-11}$	$6.3952 \times 10^{-13}$	$2.0083 \times 10^{-14}$	$6.2912 \times 10^{-16}$	$1.9697 \times 10^{-17}$	$7.7531 \times 10^{-19}$
$NE_{(n)}^{NA(5)}$	$2.2718 \times 10^1$	$2.2722 \times 10^1$	$2.2722 \times 10^1$	$2.2722 \times 10^1$	$2.2736 \times 10^1$	$2.8622 \times 10^1$

**Table 6**

[Example 4.4] The same as Table 5 for  $\gamma = 3/2$  and  $\beta = 1/2$ .

$n$	$256^2$	$512^2$	$1024^2$	$2048^2$	$4096^2$	$8192^2$
$AE_{(n)}^{NA(1)}$	$1.7841 \times 10^{-2}$	$7.5977 \times 10^{-3}$	$3.3323 \times 10^{-3}$	$1.5034 \times 10^{-3}$	$6.9661 \times 10^{-4}$	$3.2882 \times 10^{-4}$
$NE_{(n)}^{NA(1)}$	4.5852	3.8976	3.4156	3.0805	2.8540	2.6940
$AE_{(n)}^{NA(2)}$	$1.1651 \times 10^{-2}$	$4.1313 \times 10^{-3}$	$1.4628 \times 10^{-3}$	$5.1755 \times 10^{-4}$	$1.8305 \times 10^{-4}$	$6.4734 \times 10^{-5}$
$NE_{(n)}^{NA(2)}$	$4.8002 \times 10^1$	$4.8002 \times 10^1$	$4.8002 \times 10^1$	$4.8003 \times 10^1$	$4.8004 \times 10^1$	$4.8006 \times 10^1$
$AE_{(n)}^{NA(3)}$	$7.8495 \times 10^{-6}$	$1.6545 \times 10^{-6}$	$3.5619 \times 10^{-7}$	$7.2938 \times 10^{-8}$	$1.4523 \times 10^{-8}$	$3.2939 \times 10^{-9}$
$NE_{(n)}^{NA(3)}$	8.3114	9.8618	$1.1981 \times 10^1$	$1.3861 \times 10^1$	$1.5603 \times 10^1$	$2.0013 \times 10^1$

**Table 7**

[Example 4.4] The same as Table 5 for  $\gamma = 2$  and  $\beta = 1$ .

$n$	$256^2$	$512^2$	$1024^2$	$2048^2$	$4096^2$	$8192^2$
$AE_{(n)}^{NA(1)}$	$3.3144 \times 10^{-2}$	$1.6468 \times 10^{-2}$	$8.2077 \times 10^{-3}$	$4.0972 \times 10^{-3}$	$2.0470 \times 10^{-3}$	$1.0231 \times 10^{-3}$
$NE_{(n)}^{NA(1)}$	$8.5180 \times 10^0$	$8.4480 \times 10^0$	$8.4129 \times 10^0$	$8.3952 \times 10^0$	$8.3864 \times 10^0$	$8.3820 \times 10^0$
$AE_{(n)}^{NA(2)}$	$7.3264 \times 10^{-4}$	$1.8392 \times 10^{-4}$	$4.6075 \times 10^{-5}$	$1.1531 \times 10^{-5}$	$2.8842 \times 10^{-6}$	$7.2123 \times 10^{-7}$
$NE_{(n)}^{NA(2)}$	$4.8390 \times 10^1$	$4.8401 \times 10^1$	$4.8407 \times 10^1$	$4.8411 \times 10^1$	$4.8412 \times 10^1$	$4.8413 \times 10^1$
$AE_{(n)}^{NA(3)}$	$6.7224 \times 10^{-7}$	$8.4589 \times 10^{-8}$	$1.0609 \times 10^{-8}$	$1.3283 \times 10^{-9}$	$1.6617 \times 10^{-10}$	$2.0780 \times 10^{-11}$
$NE_{(n)}^{NA(3)}$	$1.1411 \times 10^1$	$1.1420 \times 10^1$	$1.1424 \times 10^1$	$1.1426 \times 10^1$	$1.1428 \times 10^1$	$1.1428 \times 10^1$

### 5. Conclusions, perspectives, and open problems

The eigenvalues of Toeplitz matrices  $T_n(f)$  with a real-valued symbol  $f$ , satisfying some conditions and tracing out a simple loop over the interval  $[-\pi, \pi]$ , are known to admit an asymptotic expansion with the form

$$\lambda_j(T_n(f)) = f(\sigma_{j,n}) + \sum_{\ell=1}^{m-1} c_\ell(\sigma_{j,n})h^{\ell\beta} + O(h^{m\beta}),$$

for some natural number  $m$ ,  $\beta \in (0, 1]$ ,  $h = 1/(n + 1)$ ,  $\sigma_{j,n} = \pi_j h$ , and where  $c_\ell$  are some bounded coefficients depending only on  $f$ . In practice, the latter expansion is numerically observed under the only condition of monotonicity and the even character of the generating function [4].

In this article we have investigated the superposition caused over this expansion, when considering a linear combination of symbols and, from a theoretical point of view, we stress that this is the first time that an eigenvalue expansion is theoretically obtained for a Toeplitz matrix-sequence with a symbol depending on  $n$ . As a further relevant contribution we have improved the precision of the algorithm in [3], by using analytic information obtained in our theoretical findings.

The problem has noteworthy applications in the differential setting, when the coefficients of the linear combination are given functions of  $h$ : in particular, by using the new expansions, we can give matrix-less eigensolvers for large matrices stemming from the numerical approximation of standard differential operators and distributed order fractional differential equations. We notice that the present approach can be viewed also as a successful application of the notion of GLT momentary symbols, a quite new research line discussed in [12,18].

It remains the open question of determining the value of  $m$  as a function of the generating function. Indeed when considering distributed fraction differential equations, it is both of interest the case where  $m$  is fixed with respect to the matrix size  $n$  and the more difficult case where  $m = m(n)$  [8–10]. Given the technical work involved, especially when  $m = m(n)$ , these generalizations will be considered in a near future.

As further developments we will consider

- a professional code in the spirit of matrix-less algorithms, also of highly parallel type;
- an extension of the theory to the case of Hermitian even matrix-valued symbols, using the basic study in [20], with the idea of treating in full generality matrix-sequences stemming from Finite Elements and IgA approximations of coercive differential problems (see also [32,55,56] and references therein);
- the case where the monotonicity is violated, which seems to be a very challenging setting, as widely discussed in [4];
- the case of variable coefficient differential operators, as a test of the notion of GLT momentary symbols (Definition 1.2) in full generality: an example of interest in applications would be the extension of the techniques to the case of operators as those in equation (1.7) with  $\alpha_s(x)$  being Riemann integrable functions, for  $s = 0, 1, \dots, s$ . Under these conditions the related matrix-sequences are not of Toeplitz type any longer, but they belong to the GLT class and admit GLT momentary symbols, in accordance with Definition 1.2.

## Declaration of competing interest

The authors declare that they have no conflict of interest.

## Data availability

Data sharing not applicable to this article as no datasets were generated or analyzed during the current study.

## Acknowledgements

The first author was supported by Universidad del Valle. Part of the numerical experiments were calculated in the computer center Jürgen Tischer of the mathematics department at Universidad del Valle. The second author was partially supported by the CONACYT project “Ciencia de Frontera” FORDECYT-PRONACES/61517/2020 and by Regional Mathematical Center of the Southern Federal University with the support of the Ministry of Science and Higher Education of Russia, Agreement 075-02-2023-924. The work of the third author is partially supported by Gruppo Nazionale per il Calcolo Scientifico (GNCS-INdAM). Furthermore, the work of Stefano Serra-Capizzano was funded from the European High-Performance Computing Joint Undertaking (JU) under grant agreement No 955701. The JU receives support from the European Union’s Horizon 2020 research and innovation programme and Belgium, France, Germany, Switzerland. Finally Stefano Serra-Capizzano is grateful for the support of the Laboratory of Theory, Economics and Systems – Department of Computer Science at Athens University of Economics and Business.

## References

- [1] M. Bogoya, A. Böttcher, S.M. Grudsky, E.A. Maximenko, Eigenvalues of Hermitian Toeplitz matrices with smooth simple-loop symbols, *J. Math. Anal. Appl.* 422 (2) (2015) 1308–1334.
- [2] M. Bogoya, S.M. Grudsky, E.A. Maximenko, Eigenvalues of Hermitian Toeplitz matrices generated by simple-loop symbols with relaxed smoothness, *Oper. Theory, Adv. Appl.* 259 (2017) 179–212.
- [3] S.-E. Ekström, C. Garoni, A matrix-less and parallel interpolation-extrapolation algorithm for computing the eigenvalues of preconditioned banded symmetric Toeplitz matrices, *Numer. Algorithms* 80 (2019) 819–848.
- [4] S.-E. Ekström, C. Garoni, S. Serra-Capizzano, Are the eigenvalues of banded symmetric Toeplitz matrices known in almost closed form?, *Exp. Math.* 27 (4) (2018) 478–487.
- [5] P. Ciarlet, *The Finite Element Method for Elliptic Problems*, Classics in Applied Mathematics, vol. 40, Society for Industrial and Applied Mathematics (SIAM), 2002, reprint of the 1978 original.
- [6] J. Cottrell, T. Hughes, Y. Bazilevs, *Isogeometric Analysis: Toward Integration of CAD and FEA*, John Wiley & Sons, 2009.
- [7] J. Strikwerda, *Finite Difference Schemes and Partial Differential Equations*, Brooks/Cole Mathematics Series, The Wadsworth, Pacific Grove, 1989.
- [8] M. Abbaszadeh, Error estimate of second-order finite difference scheme for solving the Riesz space distributed-order diffusion equation, *Appl. Math. Lett.* 88 (2019) 179–185.
- [9] M. Bogoya, S.M. Grudsky, S. Serra-Capizzano, Fast non-Hermitian Toeplitz eigenvalue computations, joining matrix-less algorithms and FDE approximation matrices, *SIAM J. Matrix Anal. Appl.* 45 (1) (2024) 284–305.
- [10] M. Mazza, S. Serra-Capizzano, M. Usman, Symbol-based preconditioning for Riesz distributed-order space-fractional diffusion equations, *Electron. Trans. Numer. Anal.* 54 (2021) 499–513.
- [11] M. Bogoya, S.-E. Ekström, S. Serra-Capizzano, Fast Toeplitz eigenvalue computations joining interpolation-extrapolation matrix-less algorithms and simple-loop theory, *Numer. Algorithms* 91 (4) (2022) 1653–1676.



- [12] M. Bolten, S.-E. Ekström, I. Furci, S. Serra-Capizzano, A note on the spectral analysis of matrix-sequences via GLT momentary symbols: from all-at-once solution of parabolic problems to distributed fractional order matrices, *Electron. Trans. Numer. Anal.* 58 (2023) 136–163.
- [13] G. Barbarino, C. Garoni, M. Mazza, S. Serra-Capizzano, Rectangular GLT sequences, *Electron. Trans. Numer. Anal.* 55 (2022) 585–617.
- [14] G. Barbarino, C. Garoni, S. Serra-Capizzano, Block generalized locally Toeplitz sequences: theory and applications in the multidimensional case, *Electron. Trans. Numer. Anal.* 53 (2020) 113–216.
- [15] G. Barbarino, C. Garoni, S. Serra-Capizzano, Block generalized locally Toeplitz sequences: theory and applications in the unidimensional case, *Electron. Trans. Numer. Anal.* 53 (2020) 28–112.
- [16] C. Garoni, S. Serra-Capizzano, *Generalized Locally Toeplitz Sequences: Theory and Applications*, vol. I, Springer, Cham, 2017.
- [17] C. Garoni, S. Serra-Capizzano, *Generalized Locally Toeplitz Sequences: Theory and Applications*, vol. II, Springer, Cham, 2018.
- [18] M. Bolten, S.-E. Ekström, I. Furci, S. Serra-Capizzano, Toeplitz momentary symbols: definition, results, and limitations in the spectral analysis of structured matrices, *Linear Algebra Appl.* 651 (2022) 51–82.
- [19] A. Böttcher, B. Silbermann, *Introduction to Large Truncated Toeplitz Matrices*, Universitext, Springer-Verlag, New York, 1999.
- [20] S.-E. Ekström, I. Furci, S. Serra-Capizzano, Exact formulae and matrix-less eigensolvers for block banded Toeplitz-like matrices, *BIT* 58 (4) (2018) 937–968.
- [21] A. Böttcher, S.M. Grudsky, E.A. Maximenko, Inside the eigenvalues of certain Hermitian Toeplitz band matrices, *J. Comput. Appl. Math.* 233 (9) (2010) 2245–2264.
- [22] A.A. Batalshchikov, S.M. Grudsky, I.S. Malisheva, S.S. Mihalkovich, E. Ramirez de Arellano, V.A. Stukopin, Asymptotics of eigenvalues of large symmetric Toeplitz matrices with smooth simple-loop symbols, *Linear Algebra Appl.* 580 (2019) 292–335.
- [23] M. Bogoya, A. Böttcher, S.M. Grudsky, Asymptotic eigenvalue expansions for Toeplitz matrices with certain Fisher–Hartwig symbols, *J. Math. Sci.* 271 (2) (2023) 176–196.
- [24] M. Bogoya, A. Böttcher, S.M. Grudsky, E.A. Maximenko, Eigenvectors of Hermitian Toeplitz matrices with smooth simple-loop symbols, *Linear Algebra Appl.* 493 (2016) 606–637.
- [25] M. Bogoya, A. Böttcher, S.M. Grudsky, E.A. Maksimenko, Asymptotics of the eigenvalues and eigenvectors of Toeplitz matrices, *Sb. Math.* 208 (11) (2017) 4–28.
- [26] C. Garoni, C. Manni, F. Pelosi, S. Serra-Capizzano, H. Speleers, On the spectrum of stiffness matrices arising from isogeometric analysis, *Numer. Math.* 127 (2014) 751–799.
- [27] M. Bogoya, S.M. Grudsky, Asymptotics for the eigenvalues of Toeplitz matrices with a symbol having a power singularity, *Numer. Linear Algebra Appl.* 30 (5) (2023) e2496.
- [28] M. Barrera, A. Böttcher, S.M. Grudsky, E.A. Maximenko, Eigenvalues of even very nice Toeplitz matrices can be unexpectedly erratic, *Oper. Theory, Adv. Appl.* 268 (2018) 51–77.
- [29] M. Barrera, S.M. Grudsky, Asymptotics of eigenvalues for pentadiagonal symmetric Toeplitz matrices, *Oper. Theory, Adv. Appl.* 259 (2017) 51–77.
- [30] M. Barrera, S.M. Grudsky, Asymptotics of eigenvalues for Toeplitz matrices with rational symbols that have a minimum of the 4th order, *Complex Var. Elliptic Equ.* 67 (3) (2022) 556–580.
- [31] J. Stoer, R. Bulirsch, *Introduction to Numerical Analysis*, 3rd edition, Springer, 2010.
- [32] C. Garoni, H. Speleers, S.-E. Ekström, A. Reali, S. Serra-Capizzano, T. Hughes, Symbol-based analysis of finite element and isogeometric B-spline discretizations of eigenvalue problems: exposition and review, *Arch. Comput. Methods Eng.* 26 (5) (2019) 1639–1690.
- [33] M. Donatelli, M. Mazza, S. Serra-Capizzano, Spectral analysis and structure preserving preconditioners for fractional diffusion equations, *J. Comput. Phys.* 307 (2016) 262–279.
- [34] M. Donatelli, M. Mazza, S. Serra-Capizzano, Spectral analysis and multigrid methods for finite volume approximations of space-fractional diffusion equations, *SIAM J. Sci. Comput.* 40 (6) (2018) A4007–A4039.
- [35] P. Tilli, A note on the spectral distribution of Toeplitz matrices, *Linear Multilinear Algebra* 45 (2–3) (1998) 147–159.
- [36] E.E. Tyrtyshnikov, N.L. Zamarashkin, Spectra of multilevel Toeplitz matrices: advanced theory via simple matrix relationships, *Linear Algebra Appl.* 270 (1998) 15–27.
- [37] P. Tilli, Locally Toeplitz sequences: spectral properties and applications, *Linear Algebra Appl.* 278 (1–3) (1998) 91–120.
- [38] S. Serra-Capizzano, Generalized locally Toeplitz sequences: spectral analysis and applications to discretized partial differential equations, *Linear Algebra Appl.* 366 (2003) 371–402.



- [39] S. Serra-Capizzano, The GLT class as a generalized Fourier analysis and applications, *Linear Algebra Appl.* 419 (1) (2006) 180–233.
- [40] G. Barbarino, Equivalence between GLT sequences and measurable functions, *Linear Algebra Appl.* 529 (2017) 397–412.
- [41] S. Serra-Capizzano, D. Sesana, E. Strouse, The eigenvalue distribution of products of Toeplitz matrices-clustering and attraction, *Linear Algebra Appl.* 432 (2010) 2658–2687.
- [42] A. Böttcher, S.M. Grudsky, *Toeplitz Matrices, Asymptotic Linear Algebra, and Functional Analysis*, Birkhäuser Verlag, Basel, 2000.
- [43] F. Di-Benedetto, G. Fiorentino, S. Serra-Capizzano, C.G. preconditioning for Toeplitz matrices, *Comput. Math. Appl.* 25 (6) (1993) 35–45.
- [44] S. Serra-Capizzano, New PCG based algorithms for the solution of Hermitian Toeplitz systems, *Calcolo* 32 (1995) 53–176.
- [45] M. Ng, *Iterative Methods for Toeplitz Systems*, Oxford University Press, 2004.
- [46] F. Gakhov, On Riemann’s boundary value problem, *Sb. Math.* 2 (44) (1937) 673–683 (in Russian).
- [47] M. Krein, Integral equations on the half-line with a kernel depending on the difference of the arguments, *Usp. Mat. Nauk* 13 (1958) 3–120 (in Russian).
- [48] A. Böttcher, S.M. Grudsky, *Spectral Properties of Banded Toeplitz Matrices*, Society for Industrial and Applied Mathematics (SIAM), 2005.
- [49] M. Kac, W.L. Murdock, G. Szegő, On the eigenvalues of certain Hermitian forms, *J. Ration. Mech. Anal.* 2 (1953) 767–800.
- [50] W.F. Trench, Asymptotic distribution of the spectra of a class of generalized Kac–Murdock–Szegő matrices, *Linear Algebra Appl.* 294 (1999) 181–192.
- [51] W.F. Trench, Spectral decomposition of Kac–Murdock–Szegő matrices, *The selected works of William F. Trench*, [http://works.bepress.com/william\\_trench/133](http://works.bepress.com/william_trench/133), 2010.
- [52] S.V. Parter, On the extreme eigenvalues of Toeplitz matrices, *Trans. Am. Math. Soc.* 100 (1961) 263–276.
- [53] R. Chan, X. Jin, *An Introduction to Iterative Toeplitz Solvers*, Society for Industrial and Applied Mathematics (SIAM), 2007.
- [54] R. Chan, M. Ng, Conjugate gradient methods for Toeplitz systems, *SIAM Rev.* 38 (3) (1996) 427–482.
- [55] M. Donatelli, C. Garoni, C. Manni, S. Serra-Capizzano, H. Speleers, Robust and optimal multi-iterative techniques for IgA Galerkin linear systems, *Comput. Methods Appl. Mech. Eng.* 284 (2015) 230–264.
- [56] S.-E. Ekström, I. Furci, C. Garoni, C. Manni, S. Serra-Capizzano, H. Speleers, Are the eigenvalues of the B-spline isogeometric analysis approximation of  $-\Delta u = \lambda u$  known in almost closed form?, *Numer. Linear Algebra Appl.* 25 (5) (2018) e2198.